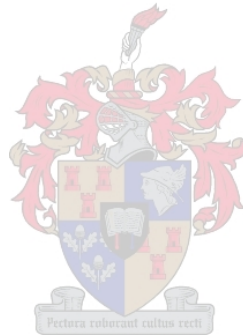


One-dimensional fluid model with oscillating, exponentially decaying pair interactions

by

Gcina Maziya



*Thesis presented in partial fulfilment of the requirements for the
degree of Master of Science in Physics in the Faculty of Science at
Stellenbosch University*

Supervisor: Prof. Michael Kastner

December 2015

The financial assistance of the National Research Foundation (NRF) towards this research is hereby acknowledged. Opinions expressed and conclusions arrived at, are those of the author and are not necessarily to be attributed to the NRF.

Declaration

By submitting this thesis electronically, I declare that the entirety of the work contained therein is my own, original work, that I am the sole author thereof (save to the extent explicitly otherwise stated), that reproduction and publication thereof by Stellenbosch University will not infringe any third party rights and that I have not previously in its entirety or in part submitted it for obtaining any qualification.

Date: December 2015

Copyright © 2015 Stellenbosch University
All rights reserved.

Abstract

One-dimensional fluid model with oscillating, exponentially decaying pair interactions

Gcina Maziya

*Department of Physics,
Stellenbosch University,*

Private Bag X1, Matieland 7602, South Africa.

Thesis: MSc. (Theoretical Physics)

December 2015

For a one-dimensional fluid model where the pair interaction potential between the molecules consists of a hard core and an exponential attraction, Kac has shown that the partition function can be determined exactly in the thermodynamic limit (Kac, 1959). Kac concluded (after the necessary calculations) that there is no phase transition for such a system with the defined pair interaction potential. The aim of this study is to investigate the phase transition with a modified potential. Therefore we repeated part of the calculations of Kac up to the derivation of the so-called Kac integral equation (see, Appendix A). This enabled us to generalise the potential function of Kac to obtain a one-dimensional fluid model with oscillating, exponentially decaying pair interactions. We then used the generalised potential to calculate the canonical partition function and obtained a modified version of the Kac integral equation. Unfortunately, we were unable to compute the eigenvalues of this modified integral equation with our chosen numerical method. Since knowing the eigenvalues is the only means to decide whether such a generalised model will show a phase transition, we were unable to investigate it. We conclude the eigenvalues have to be calculated using a different numerical method.

Uittreksel

Een-dimensionele vloeistof model met ossilerende, eksponensieel dalende paar-interaksie

("One-dimensional fluid model with oscillating, exponentially decaying pair interactions")

Gcina Maziya

Departement Fisika,

Stellenbosch Universiteit ,

Privaatsak X1, Matieland 7602, Suid-Afrika.

Tesis: MSc. (Teoretiese Fisika)

Desember 2015

Kac (Kac, 1959) het gewys dat vir 'n een-dimensionele vloeistof model waar die paar-interaksie tussen die molekules bestaan uit 'n harde kern asook 'n eksponensieel aantrekkende deel bestaan, die partisiefunksie eksak in die termodinamiese limiet bereken kan word. Die gevolgtrekking van Kac se studie is dat daar nie 'n fase oorgang vir 'n sisteem met die tipe potensiaal bestaan nie. In hierdie studie ondersoek ons die fase oorgang met 'n veralgemeende potensiaal. Dus het ons die berekeninge in Kac se artikel tot en met die afleiding van die sogenaamde Kac integraal vergelyking herhaal (sien Byvoegsel A). Dit stel ons in staat om die Kac se potensiaalfunksie te veralgemeen na 'n model vir 'n een-dimensionele vloeistof met 'n ossilerende, eksponensieel dalende paar-interaksie tussen die molekules. Ons het toe die veralgemeende potensiaal gebruik om 'n gemodifiseerde weergawe van die Kac integraal vergelyking te bereken. Ongelukkig kon ons nie die eiewaardes van die gemodifiseerde integraal vergelyking met ons gekose numeriese metode bereken nie. Omdat die eiewaardes die enigste manier is om te bepaal of die fase oorgang sal plaasvind, al dan nie, kan ons ons nie daarvoor uitspreek nie. Ons kon tot die gevolgtrekking dat die eiewaardes met 'n ander numeriese metode bereken sal moet word.

Acknowledgements

I am very grateful to my supervisor, Prof. Michael Kastner for his enormous contribution to the success of my thesis project. He inspired and guided me throughout the project, and I have no doubt I've learned a lot under his supervision. I would like to thank the University of Stellenbosch for affording me such a stimulating environment for my studies, which made it possible for me to finish my project on time. I would also like to thank the National Research Foundation (NRF) for funding my research project. Last, but not least, I would like to thank my family and friends for encouraging me during the period of my research.

Dedications

To my family

Contents

Declaration	ii
Abstract	iii
Uittreksel	iv
1 Introduction	1
1.1 Motivation	1
1.2 Introduction	2
1.3 Example: Transfer Matrix in the Ising Model	5
1.4 Why this project?	8
2 Fluid Model and Partition Function	10
2.1 A One-dimensional Fluid Model	10
2.2 Canonical Partition Function	11
3 Discretization of Integral Equation	16
3.1 Example 1:	17
3.2 Example 2:	20
4 Numerical Results and Analysis	24
4.1 Numerical integration in two-dimensions	24
4.2 Computation of eigenvalues	25
4.3 Comment on the matrix size	25
4.4 Sparse Matrix Method and Results	27
5 Conclusion	29
A Kac Integral Equation	31

Contents	viii
A.1 Derivation of the Kac Integral Equation	31
A.2 Properties of the Kernel	37
B Hilbert-Schmidt Property of kernel	41
Appendix	31
List of References	46

Chapter 1

Introduction

1.1 Motivation

Phase transitions are ubiquitous in nature. They are usual events associated with an enormous variety of physical systems (simple fluids and mixtures of fluids, magnetic materials, metallic alloys, ferroelectric materials, superfluids and superconductors, liquid crystals, etc) (Salinas, 2013). These phenomena are not only important in natural processes, but also in industry. The simple act of transforming one state of matter or phase into another, for instance by changing temperature, has always captivated the curious mind (Nishimori and Ortiz, 2010). In that way, one can convert an uninteresting state of matter into a superconducting material with tremendous implications and applications. The Large Hadron Collider (LHC) relies on the use of superconducting magnets. Those magnets not only consume less power but most importantly can achieve an order of magnitude stronger fields than ordinary magnets, a fact that is crucial to reach high energies (Nishimori and Ortiz, 2010).

Phase and phase diagram

A phase is characterised by a thermodynamic function, typically the free energy. It can also be characterised by various physical quantities, especially important is the *order parameter*, which measures how microscopic elements constituting the macroscopic phase are ordered or in a similar state (Nishimori and Ortiz, 2010). For example, in solids atoms or molecules occupy periodic positions, in which case the spatial periodicity of molecules/atoms is the order parameter. A *thermodynamic function* is a function of a few macroscopic parameters such as the temperature and the pressure. The phase of a

macroscopic substance is determined by the values of these parameters. A *phase diagram* is a graph with those parameters as the axes, on which the phase is specified for each point (Nishimori and Ortiz, 2010).

Example: water

We are all familiar with the different phases of water (vapour, liquid and ice), and the change from one to the other. Figure 1.1 below is a phase diagram of water with parameters pressure, P and temperature, T ,

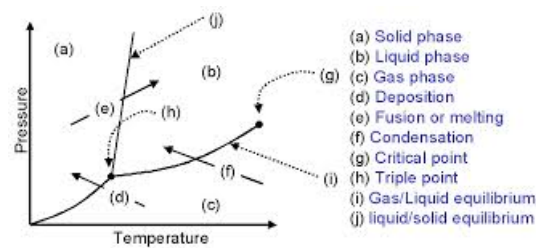


Figure 1.1: $P - T$ phase diagram for water (M. Blaber).

1.2 Introduction

The following discussion and definitions follow closely a discussion by (Kastner, 2010). Phase transitions occur both in equilibrium and nonequilibrium. In this paper we focus on a classical system at equilibrium. In the vicinity of a phase transition point, a small change in some external control parameter (such as pressure or temperature) results in a dramatic change of some physical properties (such as specific heat or electrical resistance) of the system under consideration. Also, as shown in Figure 1.2, quantities such as entropy S , the volume V , and specific heat C show some singularities as a discontinuity (jump), a *cusp* or a divergence (Nishimori and Ortiz, 2010). An example is the melting of ice, in which latent heat must be supplied to the system and consequently the entropy jumps as illustrated in Figure 1.2(a) (Nishimori and Ortiz, 2010).

From a physics stand point the reason behind the occurrence of a phase transition is the competition between the (internal) energy E and the entropy S of the system, which together determine its free energy $F = E - TS$. While the first term (E) favours order, the

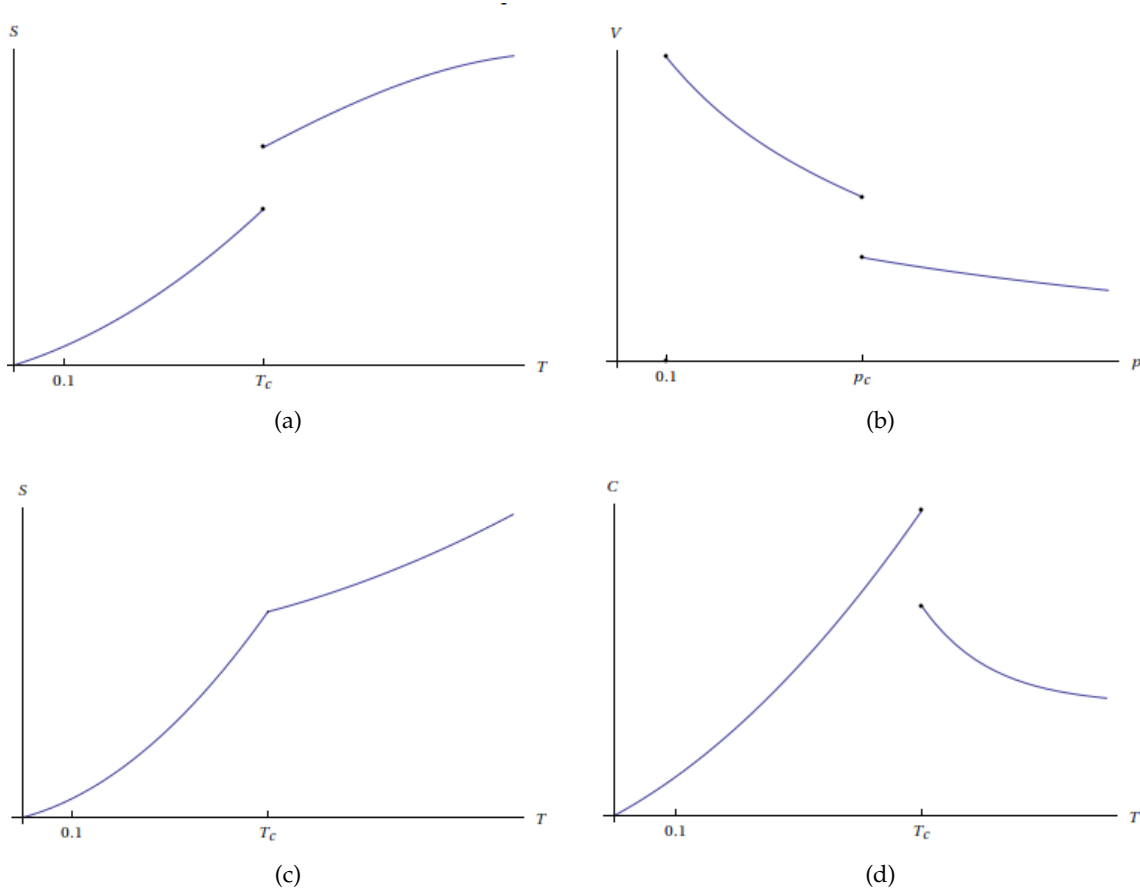


Figure 1.2: Singularities in physical quantities at transition points. S is the entropy, V is the volume and C is the specific heat. (a) and (b) are first-order transitions, and (c) and (d) are second order (Nishimori and Ortiz, 2010).

second term (S) privileges disorder, and depending on the value of the external parameters (such as T), one of the two terms dominates (Nishimori and Ortiz, 2010).

Thermodynamic description of phase transitions

In this theoretical description of phase transitions in the framework of thermodynamics, the abrupt changes of physical properties motivate the following definition (Kastner, 2010).

To capture a phase transition of interest with the above definition, the free-energy density has to be considered as a function of the relevant control parameters, i.e., those

which, upon variation, give rise to the phase transition. For the phase transition between the aggregate states of, say, water, the (Gibbs) free-energy density as a function of temperature and pressure is a suitable choice. The example that we will use to illustrate the application of the definition of a phase transition using the “*transfer*” *matrix method* is a spin system where we have two relevant control parameters, the temperature T and an external magnetic field h , and since we can replace β and h by other parameters, we therefore prefer to use the language of spin systems. Therefore, we will consider the free-energy density $\bar{f}(\beta, h)$ as a function of the inverse temperature $\beta = 1/(k_B T)$ and the magnetic field h , where k_B is the Boltzmann’s constant and T is the absolute temperature.

Quantities such as the specific heat or caloric curves which are typically measured in an experiment are then given in terms of derivatives of the free-energy density. Non-analyticities of \bar{f} may hence lead to discontinuities or divergences in these quantities, which are experimental hallmarks of phase transitions.

Definition 1.2.1. *An equilibrium phase transition is defined as a nonanalyticity of the free energy density \bar{f} .*

Statistical-physical description of phase transitions

What is the microscopic “*origin*” of a (macroscopic) phase transition? Statistical mechanics provides the microscopic foundations of thermodynamics. The starting point of such a description is a Hamiltonian function (since we are dealing with a classical system here), characterising the interactions between all elementary constituents of a physical system. The Hamiltonian function is given by

$$H(p, q) = E(p; q) - hM(p; q) \quad (1.2.1)$$

defined in phase space, where $p = (p_1, \dots, p_N)$ is the vector of momenta and $q = (q_1, \dots, q_N)$ is the vector of position coordinates.

Contact with the thermodynamic description is made by defining the canonical free energy of a system of N degrees of freedom as

Definition 1.2.2. *The canonical free-energy density (in the thermodynamic limit, i.e., $V, N \rightarrow \infty$ and $\rho = V/N = \text{constant}$) is*

$$\bar{f}(\beta, h) = \lim_{\substack{N, V \rightarrow \infty \\ \rho = \text{constant}}} -\frac{1}{N\beta} \ln Z_N(\beta, h), \quad (1.2.2)$$

where

$$Z_N(\beta, h) = \int dp dq e^{-\beta H(p, q)}, \quad (1.2.3)$$

where the integration is done over phase space. So, our definition for an equilibrium phase transition in this context is as follows

Definition 1.2.3. *An equilibrium phase transition is defined as a nonanalyticity of the canonical free-energy density \bar{f}*

1.3 Example: Transfer Matrix in the Ising Model

Here we discuss the transfer matrix method for two reasons: (1) it will serve as an example for one of the methods of computing the partition function, and (2) it has a similar feature as the method we are going to use in this paper, they both express the partition function in terms of the largest eigenvalue of the transfer matrix or (integral operator in our case). The Ising model will be our testing ground for the definition of a phase transition.

Spin- $\frac{1}{2}$ Ising model

Spin- $\frac{1}{2}$ particles can have only one of two projections along the z -axis, either up or down (usually denoted $s_i = \pm 1$). This is one of the simplest models of an interacting many-body system, which was first introduced as a model for phase transitions in magnetic systems (Ising, 1925). Despite its simplicity, the Ising model is widely applicable because it describes many interacting two state systems (Yeomans, 1992). A classical spin variable $s_i = \pm 1$ is placed on each lattice site (one-, two-, three-dimensional lattice). The spins interact according to the Hamiltonian

$$H = -J \sum_{\langle i, j \rangle} s_i s_j - h \sum_i s_i. \quad (1.3.1)$$

where h is an external magnetic field, the *coupling interaction* J is the exchange energy: positive J and negative J favours parallel and anti-parallel alignment of spins, respectively. We have used $\langle i, j \rangle$ to indicate the restriction to nearest neighbours summation, and it counts each interaction pair once. This is known as the nearest-neighbour Ising model.

As already mentioned, we shall solve (i.e., explicitly calculate the partition function) the 1D spin- $\frac{1}{2}$ nearest-neighbour Ising model. The one dimensional lattice of N sites is a linear string of spins. A spin at site i interacts with the spin at sites $i - 1$ and $i + 1$, and for convenience the lattice is made cyclic in that $s_{N+1} = s_1$. The choice of the boundary conditions becomes irrelevant in the thermodynamic limit $N \rightarrow \infty$. Here, we have adopted the discussion by (Müller-Nedebock, 2014). The partition function is

$$\begin{aligned} Z_N &= \sum_{\{s_i\}} \exp \left[\beta J \sum_i s_i s_{i+1} + \beta h \sum_i s_i \right] \\ &= \sum_{\{s_i\}} \prod_i \exp \left[\beta J s_i s_{i+1} + \frac{\beta h}{2} (s_i + s_{i+1}) \right] \end{aligned} \quad (1.3.2)$$

We now define the following column and row vectors:

$$\langle s_i | = \begin{cases} (1, 0) & \text{if } s_i = +1 \\ (0, 1) & \text{if } s_i = -1 \end{cases} \quad (1.3.3)$$

$$|s_i\rangle = (\langle s_i |)^T. \quad (1.3.4)$$

From (1.3.3) we get

$$\sum_{s=+1,-1} |s\rangle \langle s| = \begin{pmatrix} 1 & 0 \\ 0 & 1 \end{pmatrix} = \mathbb{I} \quad (1.3.5)$$

Now, we define the matrix \mathbb{T} , called the *transfer matrix*, as follows:

$$\mathbb{T} = \begin{pmatrix} e^{\beta J + \beta h} & e^{-\beta J} \\ e^{-\beta J} & e^{\beta J - \beta h} \end{pmatrix}. \quad (1.3.6)$$

From (1.3.3), (1.3.5) and (1.3.6) we get

$$\exp \left[\beta J s_i s_{i+1} + \frac{\beta h}{2} (s_i + s_{i+1}) \right] = \langle s_i | \mathbb{T} | s_{i+1} \rangle, \quad (1.3.7)$$

which is the *matrix element* of the transfer matrix.

Using the above result (1.3.7), the partition function of the 1D Ising model (1.3.2) becomes

$$Z_N = \sum_{\{s_i\}} \langle s_1 | \mathbb{T} | s_2 \rangle \langle s_2 | \mathbb{T} | s_3 \rangle \cdots \langle s_N | \mathbb{T} | s_1 \rangle. \quad (1.3.8)$$

There property $s_{N+1} = s_1$ has been used in (1.3.8). Using (1.3.5) in (1.3.8) gives

$$\begin{aligned} Z_N &= \sum_{s_1 = \pm 1} \langle s_1 | \mathbb{T} | s_1 \rangle \\ &= \text{Tr} \mathbb{T}^N. \end{aligned} \quad (1.3.9)$$

Free energy

If $\lambda_+ > \lambda_-$ are the two eigenvalues of \mathbb{T} , we find

$$Z_N(\beta, h) = \lambda_+^N + \lambda_-^N \quad (1.3.10)$$

so that

$$\begin{aligned} \beta f(\beta, h) &= \lim_{N \rightarrow \infty} \frac{1}{N} \ln Z_N \\ &= \lim_{N \rightarrow \infty} \frac{1}{N} \ln \left[\lambda_+^N \left(1 + \frac{\lambda_-^N}{\lambda_+^N} \right) \right] \\ &= \ln \lambda_+. \end{aligned} \quad (1.3.11)$$

From (1.3.6) λ_+ is found to be

$$\lambda_+ = e^{\beta J} \cosh \beta h + (e^{2\beta h} (\sin \beta h)^2 + e^{-2\beta J})^{\frac{1}{2}} \quad (1.3.12)$$

This is clearly an analytic function of β and h for $0 < \beta < \infty$ and $-\infty < h < \infty$, i.e., there is no phase transition (as singularities of $f(\beta, h)$).

1.4 Why this project?

Although we have learned from the literature about the difficulties involved in the computation of the partition function, we were motivated to make the attempt after reading a paper by Mark Kac (Kac, 1959). So, what is interesting about this Kac paper? Kac proposed a one-dimensional fluid model, for which he carried out all calculations exactly¹. The model consists of N particles moving on a line of length L and interacting in pairs through a potential $V(x)$ which consists of a hard core of length δ and an exponential attraction. For this model it was possible for Kac to give an exact discussion of the partition function in the thermodynamic limit, that is, $L \rightarrow \infty, N \rightarrow \infty, l = L/N$ finite. Kac showed that in this limit the problem can be reduced to the discussion of a linear integral equation with a positive-definite Hilbert-Schmidt kernel, for which the maximum eigenvalue determines the thermodynamic potential (Gibbs free energy) of the system (Kac *et al.*, 1963). The potential is given by

$$V(x) = \begin{cases} \infty, & 0 \leq x < \delta \\ -\alpha e^{-\gamma x}, & x \geq \delta \end{cases} \quad (1.4.1)$$

describing the particles interacting in pairs, consisting of a hard core of length δ and an exponential attraction. The sad news about this model though, is that there is no phase transition. But, anyway it's a good take home message because one can not model the particular system described above with such a potential function and hope to observe a phase transition.

So, what did we do? We first started by reproducing the results by Kac, particularly the computation of the partition function (see, Appendix A) and further computed (numerically) the eigenvalues of a certain integral equation, something which he didn't do in his paper. But, as expected the results agreed with the analytical results found by Kac. Part of the mentioned computations and results are in Appendix² A.

¹Kac has shown that the partition function can be determined exactly in the thermodynamic limit. But his model didn't show a phase transition. This model was further discussed by M. Kac, G.E. Uhlenbeck, P.C. Hemmer, they have shown that in the so-called van der Waals limit when the range of the attractive force goes to infinity while its strength becomes proportionally weaker a phase transition appears. In this paper we take a different direction, which is generalising the potential function.

²This work was done in a project that I did at the African Institute for Mathematical Sciences (AIMS <http://archive.aims.ac.za/structured-masters-research-projects/2012-13>). In the project we recovered the mentioned Kac results. But two things were not achieved, 1. the eigenvalues didn't agree with the results of Kac, more especially, when $s \rightarrow 0$ Kac proved that the largest eigenvalue, $\lambda_0 \rightarrow \infty$, while all the other eigenvalues approach finite values and 2. since the original fluid model of Kac doesn't show a phase transition we wanted to generalise it but didn't have enough time. In this project we have achieved

Remark: We have already mentioned that the partition function will be expressed in terms of eigenvalues of a certain integral equation. It is important at this stage to mention that it is these eigenvalues that are interesting since the partition function is finally expressed in terms of them and further analysis are done on the eigenvalues as we shall see in some discussion later, particularly the largest eigenvalue. We can also point out that the completely new part of this project is the computation of eigenvalues, since calculation of the partition function follows exactly the method of Kac.

We have extended and generalised the analysis of Kac by considering a more general class of potentials,

$$V(x) = \begin{cases} \infty, & 0 \leq x < \delta \\ -\alpha e^{-ax} \sin(bx + c), & x \geq \delta \end{cases} \quad (1.4.2)$$

with $a, \alpha, \delta > 0$ and $b, c \in \mathbb{R}$. These are chosen such that similar techniques of analytic calculation of the partition function can still be employed.

these two goals, with a different numerical routine from the one we used before (classified under extended formulas) we have recovered the Kac results. Thereafter we generalised the model.

Chapter 2

Fluid Model and Partition Function

2.1 A One-dimensional Fluid Model

The model we introduce is inspired and similar to the one proposed by Kac (Kac, 1959) and further discussed by Kac, Uhlenbeck, and Hemmer (Kac *et al.*, 1963).

Consider N classical particles of mass $m > 0$ on an interval of length L . The particles interact via a pair potential of the form (see also, (1.4.2))

$$V(x) = \begin{cases} \infty, & 0 \leq x < \delta \\ -\alpha e^{-ax} \sin(bx + c), & x \geq \delta \end{cases} \quad (2.1.1)$$

with $a, \alpha, \delta > 0$ and $b, c \in \mathbb{R}$.

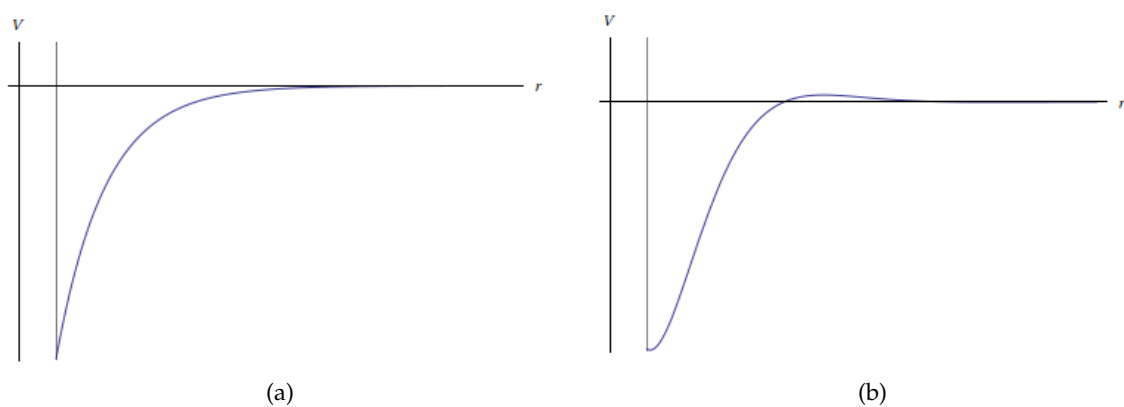


Figure 2.1: (a): Graph of the original potential considered by Kac in (Kac, 1959). (b): Modified pair potential (2.1.1)

Like in Kac's original model, V has a repulsive hard core, but in contrast to his model, an oscillating sinusoidal term is superimposed on the exponentially decaying attractive part of the pair potential (see Figure 2.1 for an illustration). The Hamiltonian function of the N -particle fluid is given by

$$H(p, q) = \sum_{i=1}^N \frac{p_i^2}{2m} + \sum_{\substack{i,j=1 \\ i \neq j}}^N V(|q_i - q_j|) \quad (2.1.2)$$

where $p = (p_1, \dots, p_N) \in \mathbb{R}^N$ denotes the vector of momenta and $q = (q_1, \dots, q_N) \in [0, L]^N$ the vector of position coordinates.

2.2 Canonical Partition Function

As mentioned in Chapter 1 and demonstrated using the example of the Ising spin chain, the problem or main goal is to compute the canonical partition function, and then the free energy density f in the thermodynamic limit,

$$\bar{f}_N(\beta, h) = \lim_{\substack{N, V \rightarrow \infty \\ \rho = \text{constant}}} -\frac{1}{N\beta} \ln Z_N(\beta, h), \quad (2.2.1)$$

where

$$Z_N(\beta, h) = \int dp dq e^{-\beta H(p, q)}, \quad (2.2.2)$$

as a function of the inverse temperature β and the density ρ , where the canonical partition function is given by

$$\begin{aligned} Z_N(\beta, L) &= \frac{1}{\Lambda^N N!} \int_0^L \cdots \int_0^L dq_1 \cdots dq_N \exp \left(-\beta \sum_{k < j} V(|q_k - q_j|) \right) \\ &= \frac{1}{\Lambda^N N!} \int_0^L \cdots \int_0^L dq_1 \cdots dq_N \prod_{k < l} S(q_k - q_l) \\ &\quad \times \exp \left(\alpha \beta \sum_{k < l} e^{-a|q_k - q_l|} \sin(b|q_k - q_l| + c) \right). \end{aligned} \quad (2.2.3)$$

Here the Gaussian p_k -integrals have already been performed, resulting in the prefactor in terms of the thermal de Broglie wavelength $\Lambda = \hbar \sqrt{2\pi\beta/m}$. The step function

$$S(r) = \begin{cases} 0 & \text{for } |r| < \delta \\ 1 & \text{for } |r| > \delta \end{cases} \quad (2.2.4)$$

in (2.2.3) takes into account the hard core repulsion of the pair potential (1.4.2). The following steps of the analysis of Z_N proceed very much along the line of the calculations in (Kac, 1959) and (Kac *et al.*, 1963) (also see, Appendix A. Since the hard core of the pair potential (1.4.2) imposes a linear order of the particles, and noting that the integrand is symmetric under permutations of q_1, \dots, q_N , we can write (2.2.3) in the form

$$\begin{aligned} Z_N(\beta, L) &= \frac{1}{\Lambda^N} \int \cdots \int_{0 \leq q_1 < \cdots < q_N \leq L} dq_1 \cdots dq_N \prod_{j=1}^{N-1} S(q_{j+1} - q_j) \\ &= \exp \left(\frac{\alpha\beta}{2} \sum_{k,l=1}^N e^{-a|q_k - q_l|} \sin(b|q_k - q_l| + c) \right). \end{aligned} \quad (2.2.5)$$

Using the exponential representation of the sine function, we obtain

$$\begin{aligned} Z_N(\beta, L) &= \frac{1}{\Lambda^N} \int \cdots \int_{0 \leq q_1 < \cdots < q_N \leq L} dq_1 \cdots dq_N \prod_{j=1}^{N-1} S(q_{j+1} - q_j) \\ &= \exp \left(\frac{\nu}{2} \sum_{k,l=1}^N e^{-\gamma|q_k - q_l|} \right) \left(\frac{\nu^*}{2} \sum_{k,l=1}^N e^{-\gamma^*|q_k - q_l|} \right) \end{aligned} \quad (2.2.6)$$

where $\nu = -ie^{-ic}\alpha\beta/2$ and $\gamma = a - ib$. Like in Kac the calculation we going to use the identity

$$\begin{aligned} \left(\frac{\nu}{2} \sum_{k,l=1}^N e^{-\gamma|q_k - q_l|} \right) &= \int_{-\infty}^{\infty} \cdots \int_{-\infty}^{\infty} dx_1 \cdots dx_N W(x_1) \exp \left(\sqrt{\nu} \sum_{k=1}^N x_k \right) \\ &\quad \times \prod_{l=1}^{N-1} P_{\gamma}(x_l | x_{l+1}, q_{l+1} - q_l) \end{aligned} \quad (2.2.7)$$

where

$$W(x) = \frac{1}{\sqrt{2\pi}} \exp \left(-\frac{x^2}{2} \right) \quad (2.2.8)$$

and

$$P_{\gamma}(x | \bar{x}, t) = \frac{1}{\sqrt{2\pi(1 - e^{-2\gamma t})}} \exp \left(-\frac{(\bar{x} - xe^{-\gamma t})^2}{2(1 - e^{-2\gamma t})} \right) \quad (2.2.9)$$

Now, using (2.2.7) in (2.2.6) we get the canonical partition function in the form of a product of nearest-neighbour pair functions in both q and x ,

$$\begin{aligned}
Z_N(\beta, L) &= \frac{1}{\Lambda^N} \int \cdots \int_{0 \leq q_1 < \cdots < q_N \leq L} dq_1 \cdots dq_N \prod_{j=1}^{N-1} S(q_{j+1} - q_j) \\
&\times \int_{-\infty}^{\infty} \cdots \int_{-\infty}^{\infty} dx_1 \cdots dx_N W(x_1) \prod_{k=1}^N \exp(\sqrt{v} x_k) \\
&\times \prod_{l=1}^{N-1} P_\gamma(x_l | x_{l+1}, q_{l+1} - q_l) \\
&\times \int_{-\infty}^{\infty} \cdots \int_{-\infty}^{\infty} dy_1 \cdots dy_N W(y_1) \prod_{k=1}^N \exp(\sqrt{v^*} y_k) \\
&\times \prod_{l=1}^{N-1} P_{\gamma^*}(y_l | y_{l+1}, q_{l+1} - q_l)
\end{aligned} \tag{2.2.10}$$

In the q variables, the integrand in (2.2.10) depends only on the difference $q_{l+1} - q_l$ of pairs of nearest neighbours. This property allows us to perform the q integrations by making a Laplace transform in L , and analogous to the calculation in Appendix A, we obtain

$$\begin{aligned}
\mathcal{Z}(\beta, s) &= \int_0^\infty dL e^{-sL} Z_N(\beta, L) \\
&= \frac{1}{\Lambda^N s^2} \int_{-\infty}^{\infty} \cdots \int_{-\infty}^{\infty} dx_1 y_1 \cdots dx_N y_N W(x_1) W(y_1) \\
&\times \exp \left(\sum_{k=1}^N \left[\sqrt{v} x_k + \sqrt{v^*} y_k \right] \right) \prod_{l=1}^{N-1} p_s(x_l, y_l; x_{l+1}, y_{l+1})
\end{aligned} \tag{2.2.11}$$

with

$$p_s(x, y; \bar{x}, \bar{y}) = \int_\delta^\infty d\tau e^{-s\tau} P_\gamma(x | \bar{x}, \tau) P_{\gamma^*}(y | \bar{y}, \tau), \tag{2.2.12}$$

where δ is the diameter of the hard core of the pair potential (1.4.2). The ordering of the x_l, y_l in successive pairs suggests the introduction of the kernel

$$K_s(x, y; \bar{x}, \bar{y}) = \frac{W(x)W(y)p_s(x, y; \bar{x}, \bar{y})}{\sqrt{W(x)W(y)W(\bar{x})W(\bar{y})}} \exp \left[\frac{\sqrt{v}(x + \bar{x}) + \sqrt{v^*}(y + \bar{y})}{2} \right] \tag{2.2.13}$$

K_s is symmetric upon exchanging (x, y) with (\bar{x}, \bar{y}) , and one can show that, for $\delta > 0$, it is a Hilbert-Schmidt kernel,

$$\int \int \int \int_{-\infty}^{\infty} d\bar{x} d\bar{y} |K_s(x, y; \bar{x}, \bar{y})|^2 < \infty \tag{2.2.14}$$

The proof of (2.2.14) is shown in Appendix B. Property (2.2.14) implies that the integral operator \mathcal{K}_s defined by

$$(\mathcal{K}_s \psi)(x, y) = \int \int_{-\infty}^{\infty} d\bar{x} d\bar{y} K_s(x, y; \bar{x}, \bar{y}) \psi(\bar{x}, \bar{y}) \quad (2.2.15)$$

is a Hilbert-Schmidt operator in the space $L^2(\mathbb{R})$ of square-integrable functions on the real plane. Therefore, \mathcal{K}_s has a complete set of orthonormal eigenfunctions $\psi_j(x, y; s)$ with discrete eigenvalues $\lambda_j(s)$ for $j = 0, 1, 2, \dots$, satisfying the integral equation

$$\int \int_{-\infty}^{\infty} d\bar{x} d\bar{y} K_s(x, y; \bar{x}, \bar{y}) \psi_j(\bar{x}, \bar{y}; s) = \lambda_j(s) \psi_j(x, y; s) \quad (2.2.16)$$

Accordingly, the kernel K_s can be expanded in the convergent series

$$K_s(x, y; \bar{x}, \bar{y}) = \sum_{j=0}^{\infty} \lambda_j(s) \psi_j(x, y; s) \psi_j^*(\bar{x}, \bar{y}; s) \quad (2.2.17)$$

The Laplace transform of the partition function \mathcal{Z}_N in (2.2.11) can be expressed in terms of K_s by writing

$$\begin{aligned} \mathcal{Z}_N(\beta, s) &= \frac{1}{\Lambda^{N_S^2}} \int_{-\infty}^{\infty} dx_1 dy_1 \cdots dx_N dy_N \\ &\times \sqrt{W(x_1)W(y_1)W(x_N)W(y_N)} \exp \left[\frac{\sqrt{v}(x_1 + x_N) + \sqrt{v^*}}{2} \right] \\ &\times \prod_{l=1}^{N-1} K_s(x_l, y_l; x_{l+1}, y_{l+1}) \end{aligned} \quad (2.2.18)$$

The Hilbert-Schmidt property of the kernel K_s allows us to express \mathcal{Z}_N in terms of the eigenvalues and eigenfunctions of the integral operator \mathcal{K}_s . Inserting the series expansion (2.2.17) into (2.2.18) and integrating over $x_2, y_2, \dots, x_{N-1}, y_{N-1}$ (calculation similar to that of Equations (A.2.5) - (A.2.10) in Appendix A), we obtain

$$\mathcal{Z}_N(\beta, s) = \frac{1}{\Lambda^{N_S^2}} \sum_{j=0}^{\infty} \lambda_j^{N-1}(s) A_j \bar{A}_j \quad (2.2.19)$$

with

$$A_j = \int \int_{-\infty}^{\infty} dx dy \psi_j(x, y; s) \sqrt{W(x)W(y)} \exp \left[\frac{\sqrt{v}x + \sqrt{v^*}y}{2} \right] \quad (2.2.20)$$

$$\bar{A}_j = \int \int_{-\infty}^{\infty} dx dy \psi_j^*(x, y; s) \sqrt{W(x)W(y)} \exp \left[\frac{\sqrt{v}x + \sqrt{v^*}y}{2} \right] \quad (2.2.21)$$

From (2.2.19) above we have that the calculation of \mathcal{Z} , which the Laplace transform of Z , has been reduced to the calculation of eigenvalues and eigenvectors of K_s (see also (2.2.16) above). The computation of these eigenvalues and eigenvectors of K_s is extremely difficult if not impossible. This implies we have to do the computation numerically, which is almost always possible if K is well behaved. In the next Chapter we develop the numerical method to do the mentioned task.

Chapter 3

Discretization of Integral Equation

The fact that integrals of elementary functions could not, in general, be computed analytically, gave birth to numerical integration, also called quadrature (Flannery *et al.*, 1992). Firstly, we want to discuss the quadrature method we have adopted to evaluate the integral

$$I = \int_a^b f(x)dx. \quad (3.0.1)$$

This quadrature method is based on the obvious strategy of adding up the value of the integrand at a sequence of abscissas within the range of integration. The game is to obtain the integral as accurately as possible with the smallest number of function evaluations of the integrand (Flannery *et al.*, 1992). It is very important for us to describe the quadrature method we have used to evaluate (3.0.1) because it is the method we are going to use for the numerical integration in this paper. We are going to explain how.

The quadrature method we are going to use is classified under the so-called extended formulas¹ (for more details, see (Flannery *et al.*, 1992)). It is given by

¹In previous work done when at AIMS the Gauss-Hermite quadrature method was used. But this method did not work, i.e., we couldn't recover the eigenvalues as proved by Kac. This problem was solved by using the above discretization method, where the eigenvalues converged and behaved as proved by Kac.

$$\begin{aligned} & \int_{a=x_1}^{b=x_N} dx f(x) \\ &= \Delta x \left[\frac{3}{8}f_1 + \frac{7}{6}f_2 + \frac{23}{24}f_3 + f_4 + \cdots + f_{N-3} + \frac{23}{24}f_{N-2} + \frac{7}{6}f_{N-1} + \frac{3}{8}f_N \right] \\ &+ O\left(\frac{1}{N^4}\right), \end{aligned} \quad (3.0.2)$$

where $x_1, x_2, \dots, x_{N-1}, x_N$, is a sequence of abscissas which are spaced apart by a constant step $\Delta x = \frac{b-a}{N}$.

$$x_i = x_1 + i\Delta x, i = 1, 2, \dots, N.$$

A function $f(x)$ has known values at the x_i 's,

$$f(x_i) \equiv f_i.$$

3.1 Example 1:

Now, we are ready to apply our quadrature (3.0.2). The problem to which we apply our quadrature is an eigenvalue problem, which has (1) an exact solution: which shows how accurate the quadrature is and (2) it serves as a first step to the solution of our problem: since we are also going to solve an eigenvalues problem. So, this example is very important for those two reasons. It is the homogeneous Fredholm equation of the second kind (for details on Fredholm equations, see (Masujima, 2005)), which is Exercise 4.9 on page 102 of the book (Masujima, 2005) and is given by

$$\lambda \int_{-\infty}^{\infty} dy K(x, y) \phi(y) = \phi(x), \quad -\infty < x < \infty, \quad (3.1.1)$$

which can be rewritten (with $\lambda \rightarrow \frac{1}{\lambda}$, since λ is just a constant) as

$$\int_{-\infty}^{\infty} dy K(x, y) \phi(y) = \lambda \phi(x), \quad -\infty < x < \infty, \quad (3.1.2)$$

where

$$K(x, y) = \frac{1}{\sqrt{1-t^2}} \exp\left[\frac{x^2 + y^2}{2}\right] \exp\left[-\frac{x^2 + y^2 - 2xyt}{1-t^2}\right] \quad (3.1.3)$$

with t fixed and $0 < t < 1$.

3.1.1 Analytical Results

The integral equation (3.1.3) has eigenvalues

$$\lambda_n = \sqrt{\pi} t^n, \quad n = 0, 1, 2, \dots \quad (3.1.4)$$

Below is a table for the first five eigenvalues, that is, λ_n for $n = 0, 1, 2, \dots, 4$.

n	λ_n	t=0.2	t=0.4	t=0.6	t=0.8
0	λ_0	1.77245000	1.7724500	1.772450	1.772457
1	λ_1	0.35449100	0.7089820	1.063470	1.417960
2	λ_2	0.07089820	0.2835930	0.638083	1.134370
3	λ_3	0.01417960	0.1134370	0.382850	0.907496
4	λ_4	0.00283593	0.0453748	0.229710	0.725997

Table 3.1: First five eigenvalues, λ_n , for $n = 0, 1, 2, \dots, 4$, which were computed from (3.1.4). This eigenvalues will be compared to the numerically ones computed using (3.0.2)

3.1.2 Numerical results

Now, we want to use our quadrature method to compute the eigenvalues of the integral equation (3.1.2) and compare the results with that in Table 3.1 above. Equation (3.1.2) has limits $-\infty$ to ∞ , which means it is an improper integral (Masujima, 2005). In order to apply (3.0.2) we need (3.1.2) to have finite limits. This can be done by noting that, outside a certain range the value of $K(x, y)$ is essentially zero (see, Fig.3.1) . below).

The integral equation (3.1.2) becomes

$$\Delta y \sum_{i=1}^N K(x, y_i) \phi(y_i) = \lambda \phi(x). \quad (3.1.5)$$

We choose discrete x values in such a way that $x_i = y_i$, so that (3.1.5) written as a system of linear equations becomes

$$\Delta y \begin{pmatrix} w_1 K(x_1, y_1) & \cdots & w_N K(x_1, y_N) \\ w_1 K(x_2, y_1) & \cdots & w_N K(x_2, y_N) \\ \vdots & & \vdots \\ w_1 K(x_N, y_1) & \cdots & w_N K(x_N, y_N) \end{pmatrix} \begin{pmatrix} \phi(y_1) \\ \phi(y_2) \\ \vdots \\ \phi(y_N) \end{pmatrix} = \lambda \begin{pmatrix} \phi(x_1) \\ \phi(x_2) \\ \vdots \\ \phi(x_N) \end{pmatrix} \quad (3.1.6)$$

which is the standard eigenvalue problem and *Mathematica* has been used to compute the eigenvalues for $N = 15$, $N = 20$ and $N = 25$ to obtain the first five eigenvalues

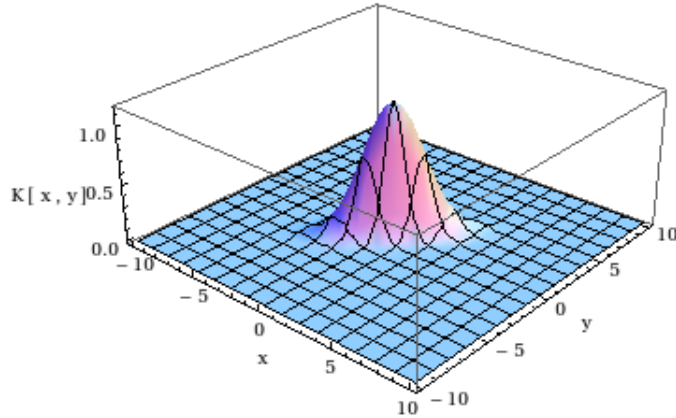


Figure 3.1: The plot of the kernel $K(x, y)$, Equation(3.1.3) for $t = 0.5$. We can see that for $(x, y) = (-10, -10)$ or $(x, y) = (10, 10)$, for example, the kernel is almost zero. So, we can choose our bounds to be $-10 < x, y < 10$, and it can be shown that increasing this bounds to $-15 < x, y < 15$, for instance, would not affect the results.

which are tabulated below. This was done for the cases $t = 0.2$ and $t = 0.8$. $N = 15$, $N = 20$ and $N = 25$ was done to check convergence of the eigenvalues, and we can clearly see that the eigenvalues indeed converge,

λ_n	t=0.2(N=20)	t=0.2(N=30)	t=0.2(N=40)	t=0.8(N=20)	t=0.8(N=30)	t=0.8(N=40)
λ_0	1.7719800	1.77245000	1.77245000	1.876730	1.7733400	1.772450
λ_1	0.3512500	0.35449100	0.35449100	1.615700	1.4201400	1.417970
λ_2	0.0685784	0.07089800	0.07089820	1.314660	1.1385400	1.134380
λ_3	0.0162239	0.01417990	0.01417960	1.285860	0.9145620	0.907520
λ_4	0.0018360	0.00283548	0.00283593	0.802914	0.7367960	0.726042

Table 3.2: First five eigenvalues, λ_n , for $n = 0, 1, 2, \dots, 4$

As we can see from both tables above, the numerically computed eigenvalues are in good agreement with the exact ones. We also observe that, for $N = 30$ and $N = 40$ the eigenvalues have converged.

3.1.3 Error Analysis

Let us consider the case of $t = 0.2$ and $N = 50$, and compare the exact results to the numerical one, to get a quantitative idea of how close the numerical results are to the exact ones.

n	λ_n	Exact	Numerical	% Error
0	λ_0	1.77245000	1.77245000	0.000
1	λ_1	0.35449100	0.35449100	0.000
2	λ_2	0.07089820	0.07089820	0.000
3	λ_3	0.01417960	0.01417960	0.000
4	λ_4	0.00283593	0.00283593	0.000

Table 3.3: Comparing the numerical eigenvalues to the exact eigenvalues by computing the % error. For $N = 50$ discretization points, the eigenvalues have already converged to the exact ones. This shows that our discretization method is accurate, at least for the problem at hand.

3.2 Example 2:

Firstly, we have to mention that this example is very important, because it shows how the numerical integration method described above, which is for the one-dimensional case, is generalised to the two-dimensional case and then applied to a simple case with known results to check that it reproduces the same results. Now, we write the above integral equation in a generalized form, which is simply a product of the integrand, and then integrated in the plane, which becomes

$$\int_{-\infty}^{\infty} \int_{-\infty}^{\infty} dy d\bar{y} K(x, y; t) K(\bar{x}, \bar{y}; t) \psi(y) \psi(\bar{y}) = \lambda \bar{\lambda} \psi(x) \psi(\bar{x}). \quad (3.2.1)$$

Analytically, the solution is given by

$$\lambda_n = \sqrt{\pi} t^n$$

and

$$\bar{\lambda}_n = \sqrt{\pi} t^n = \lambda_n$$

for $n = 0, 1, 2, 3, \dots$. This readily gives the eigenvalues solution to (3.2.1) as

$$\lambda \bar{\lambda} = \lambda_0 \lambda_0, \lambda_0 \lambda_1, \lambda_1 \lambda_0, \lambda_0 \lambda_2, \dots \quad (3.2.2)$$

Numerically, if we apply our quadrature rule (3.0.2), we get the following system of equations

$$\begin{aligned}
& \Delta y \Delta \bar{y} \begin{pmatrix} w_0 w_0 K(x_0, y_0) K(\bar{x}_0, \bar{y}_0) & \dots & w_n w_n K(x_0, y_n) K(\bar{x}_0, \bar{y}_n) \\ w_0 w_0 K(x_1, y_0) K(\bar{x}_0, \bar{y}_0) & \dots & w_n w_n K(x_1, y_0) K(\bar{x}_n, \bar{y}_n) \\ \vdots & \ddots & \vdots \\ w_0 w_0 K(x_n, y_n) K(\bar{x}_0, \bar{y}_0) & \dots & w_n w_n K(x_n, y_n) K(\bar{x}_n, \bar{y}_n) \end{pmatrix} \begin{pmatrix} \psi(x_0) \psi(\bar{x}_0) \\ \psi(x_1) \psi(\bar{x}_0) \\ \vdots \\ \psi(x_n) \psi(\bar{x}_n) \end{pmatrix} \\
& = \lambda \begin{pmatrix} \psi(x_0) \psi(\bar{x}_0) \\ \psi(x_1) \psi(\bar{x}_0) \\ \vdots \\ \psi(x_n) \psi(\bar{x}_n) \end{pmatrix}. \tag{3.2.3}
\end{aligned}$$

It has been checked that the above generalised analytical result for the eigenvalues, $\lambda \bar{\lambda}$, agrees with the numerically computed eigenvalues using (3.2.3), but the results are not shown here.

3.2.1 Example 3: Eigenvalues for the Kac model (1D integration)

Here, we are interested in computing the eigenvalues of the following so-called Kac integral equation using (3.2.3)

$$\int_{-\infty}^{\infty} K_s(x, y) \psi(y) dy = \lambda \psi(x), \tag{3.2.4}$$

$$K_s(x, y) = \frac{W(x) p_s(x|y)}{[W(x) W(y)]^{\frac{1}{2}}} \exp \left[\frac{\nu^{\frac{1}{2}}}{2} (x + y) \right], \tag{3.2.5}$$

$$p_s(x|y) = \int_{\delta}^{\infty} \exp(-st) P(x|y; t) dt; \tag{3.2.6}$$

$$P(x|y, t) = \frac{\exp \left\{ -\frac{(y - x e^{-\gamma t})^2}{2(1 - e^{-2\gamma t})} \right\}}{[2\pi(1 - e^{-2\gamma t})]^{\frac{1}{2}}}, \tag{3.2.7}$$

with $W(x) = \frac{1}{\sqrt{2\pi}} \exp(-\frac{1}{2}x^2)$.

The plot of the above kernel, $K_s(x, y)$, is given in Figure 3.2 below

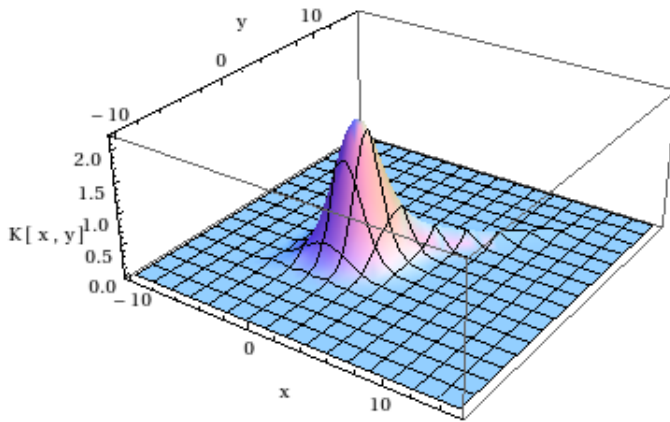


Figure 3.2: The plot of the kernel $K(x, y)$, Equation (3.2.5) for $(\delta, \nu, \gamma, s) = (0.1, 0.1, 1.0, 0.2)$. It is clear that we can choose our bounds to be $-10 < x, y < 15$.

Now, let's use (3.1.6) to compute the eigenvalues of (3.2.4). *Mathematica* was used to compute the eigenvalues and the first five eigenvalues are

n	λ_n	$N = 30$	$N = 40$	$N = 80$
1	λ_1	5.247460	5.247460	5.247460
2	λ_2	0.932509	0.932490	0.932491
3	λ_3	0.522289	0.522252	0.522253
4	λ_4	0.358080	0.358022	0.358023
5	λ_5	0.266312	0.266225	0.266227

Table 3.4: First five numerically computed eigenvalues of the Kac integral equation. This was done for different numbers of discretisation points, $N = 30$, $N = 40$ and $N = 80$. We can see that all eigenvalues converge to the first five decimal places.

3.2.2 Example 4: Eigenvalues K' 2D integration)

Now, let's consider $K'_s(x, y; \bar{x}, \bar{y}) = K_s(x, y)K(\bar{x}, \bar{y})$, for $N = 40$ discretization points. From the Table 3.4 above, the first five eigenvalues are

n	λ_n	$N = 40$
1	λ_1	27.5358
2	λ_2	4.89320
3	λ_3	4.89320
4	λ_4	2.74050
5	λ_5	2.74050

Table 3.5: First five eigenvalues computed from the eigenvalues of the generalised integral equation using the values for $N = 40$ discretization points in Table 3.4 above

Now, we have used (3.2.3) to compute the same eigenvalues. The results that we obtained are as follows

n	λ_n	$N = 40$
1	λ_1	27.5358
2	λ_2	4.89341
3	λ_3	4.89341
4	λ_4	2.73963
5	λ_5	2.73963

Table 3.6: First five eigenvalues computed from the eigenvalues of the generalised integral equation using 3.2.3. When compared to the Table 3.5 above the first three agree to three decimal places.

This is all good news. Now, we are ready to compute the eigenvalues of the integral Equation 2.2.16, which is a crucial part of this paper because it is the eigenvalues of this integral equation that will tell us whether there is a phase transition or not for our system. The examples have shown that our discretization method enables us to compute the eigenvalues to a very good approximation, at least for the two different kernels we have considered. So, we managed at least to show two important things in the computation of the eigenvalues, (1) convergence of eigenvalues, (2) agreement between eigenvalues found using the two dimensional version of the numerical integration method and the ones found by using the already computed eigenvalues of the one-dimensional integration method, at least in the two examples where we created a two dimensional version of the integral equation by simply multiplying the one-dimensional integral equation by itself.

Chapter 4

Numerical Results and Analysis

4.1 Numerical integration in two-dimensions

In general, our numerical integration in two-dimensions is

$$\int_a^b \int_a^b d\bar{x} d\bar{y} K(x, y; \bar{x}_i, \bar{y}_j; s) \psi(\bar{x}, \bar{y}) \approx \Delta \bar{x} \Delta \bar{y} \sum_{i,j=1}^N w_i w_j K(x, y | \bar{x}_i, \bar{y}_j; s) \psi(\bar{x}_i, \bar{y}_j), \quad (4.1.1)$$

which gives

$$\Delta \bar{x} \Delta \bar{y} \begin{pmatrix} w_0 w_0 K(x_0, y_0 | \bar{x}_0, \bar{y}_0; s) & \dots & w_n w_n K(x_0, y_0 | \bar{x}_n, \bar{y}_n; s) \\ w_0 w_0 K(x_1, y_0 | \bar{x}_0, \bar{y}_0; s) & \dots & w_n w_n K(x_1, y_0 | \bar{x}_n, \bar{y}_n; s) \\ \vdots & \ddots & \vdots \\ w_0 w_0 K(x_n, y_n | \bar{x}_0, \bar{y}_0; s) & \dots & w_n w_n K(x_n, y_n | \bar{x}_n, \bar{y}_n; s) \end{pmatrix} \begin{pmatrix} \psi(\bar{x}_0, \bar{y}_0) \\ \psi(\bar{x}_1, \bar{y}_0) \\ \vdots \\ \psi(\bar{x}_n, \bar{y}_n) \end{pmatrix} = \lambda \begin{pmatrix} \psi(x_0, y_0) \\ \psi(x_1, y_0) \\ \vdots \\ \psi(x_n, y_n) \end{pmatrix}, \quad (4.1.2)$$

where we set $x_i = \bar{x}_i$ and $y_j = \bar{y}_j$ so that Equation (4.1.2) becomes an eigenvalue problem as we have already mentioned before. In fact, the method we have used to compute the eigenvalues in the last examples in the Chapter 3 is indeed the one given by Equation (4.1.2)

4.2 Computation of eigenvalues

Now, we are ready to compute the eigenvalues of Equation (4.1.2) where the kernel¹ (which was derived in Chapter 2) is given by

$$K_s(x, y; \bar{x}, \bar{y}) = \frac{W(x)W(y)p_s(x, y; \bar{x}, \bar{y})}{\sqrt{W(x)W(y)W(\bar{x})W(\bar{y})}} \exp \left[\frac{\sqrt{v}(x + \bar{x}) + \sqrt{v^*}(y + \bar{y})}{2} \right] \quad (4.2.1)$$

where

$$p_s(x, y; \bar{x}, \bar{y}) = \int_{\delta}^{\infty} d\tau e^{-s\tau} P_{\gamma}(x|\bar{x}, \tau) P_{\gamma^*}(y|\bar{y}, \tau), \quad (4.2.2)$$

where δ is the diameter of the hard core of the pair potential and

$$P_{\gamma}(x|\bar{x}, t) = \frac{1}{\sqrt{2\pi(1 - e^{-2\gamma t})}} \exp \left(-\frac{(\bar{x} - xe^{-\gamma t})^2}{2(1 - e^{-2\gamma t})} \right) \quad (4.2.3)$$

where

$$W(x) = \frac{1}{\sqrt{2\pi}} \exp \left(-\frac{x^2}{2} \right). \quad (4.2.4)$$

This is done by the methods outlined in Chapter 3.

4.3 Comment on the matrix size

The matrix on the left hand side of Equation (4.1.2) above has size $n^2 \times n^2$, where n^2 is the number of discretisation points in the plane. To apply the method of Chapter 3 to this problem we need to make a few modifications or improvements. One thing

¹Unlike in the original Kac potential where we had two parameters, (a, α) , in the general case we have four control parameter (a, b, c, α) . Some of these parameters have an impact in the calculation of the kernel. a and α are the same as in the Kac case and does not affect the computation of K . c is not interesting, setting it to be zero can just as well do. The main suspect is b , which is the periodicity of the *sine* function. Computation of K have indicated that for large values of b , larger than one, *Mathematica* fails to compute K because the integration involved in this computation and integrating a highly oscillatory function can be problematic.

that you should have suspected already is, for what n does the eigenvalues of Equation (4.1.2) converge since, for example, when $n = 20$ the size of the matrix is 400×400 ? It turns out that this very question is the stumbling block to the success of the computation of the eigenvalues.

What we did at first was to simply use the method developed in Chapter 3 to compute the eigenvalues. Although the computation was very slow for a small number of discretization points such as $n = 20$, we did get some eigenvalues. We have already asked the question, did the eigenvalues converge for $n = 20$, for instance?, and if they didn't, then how long is it going to take *Mathematica* to compute the eigenvalues for $n = 30$? Yes, it is slow, but what we found out is that we can go up to $n = 70$ and get the eigenvalues within a day. For $n = 80$, for which the matrix size is 6400×6400 , *Mathematica* couldn't store the elements of the matrix. This was a huge blow because the eigenvalues have not converged yet.

So, how do we get out of this situation? We realised that our kernel has the same features as the kernel in Figure 3.1, it is mostly non-zero along the diagonal of the domain and effectively zero as you go away from the diagonal. So, we can cleverly² chose a number $\eta \in \mathbb{R}$, such that

$$K'(x, y; \bar{x}, \bar{y}) = \begin{cases} K(x, y; \bar{x}, \bar{y}) & \text{if } |x - \bar{x}| > \eta \text{ or } |y - \bar{y}| > \eta, \\ 0 & \text{otherwise.} \end{cases} \quad (4.3.1)$$

This is, in fact, all we needed because instead of computing K for the matrix elements, we are going to compute K' which will increase the speed of the computation of the matrix elements since for $K' = 0$ no computation is going to be done and *Mathematica* will only store in its memory the non-zero elements of the matrix and everything else will be taken care of by using the Sparse matrix method in *Mathematica*. We have checked for $n = 20$ that *Mathematica* gives the same results when using K' as illustrated in Table 4.1 This is going to allow us to increase the number of discretisation points and hope that the eigenvalues will converge. We will call the method of computing the eigenvalues using K' the *Sparse Matrix Method*.

²What we mean by this, is that for a given set of parameters, we compute enough values of K on a grid in \mathbb{R}^4 and then it is after we have computed these values of K that we are in a better position to chose in which regions of the domain \mathbb{R}^4 to set $K = 0$. The choice of the integration domain, i.e., setting the limits of integration, pops up in a similar manner.

λ_n	Kernel: is K	Kernel: is K'
λ_1	$37176.7 + 6.66076 \times 10^{-12}i$	$37176.7 + 6.66076 \times 10^{-12}i$
λ_2	$15265.7 - 31449.2i$	$15265.7 - 31449.2i$
λ_3	$15265.7 + 31449.2i$	$15265.7 + 31449.2i$
λ_4	$33415.5 + 2.18279 \times 10^{-11}i$	$33415.5 + 2.18279 \times 10^{-11}i$
λ_5	$15673.8 + 29234.2i$	$15673.8 + 29234.2i$

Table 4.1: First five eigenvalues, λ_n , for $n = 1, 2, \dots, 5$. This is for the original kernel K and the modified kernel K' . We can see from the table the the eigenvalues are the same. So, our modified kernel indeed gives the same results as the original kernel, but the former has the advantage that it can be fast and can be computed for large number of discretisation points as compared to the latter.

The following section will give the results of this method, from which we will conclude whether the eigenvalues converge or not. As we have mentioned before, the rest of the analysis, including the discussion of the physics of the model, in particular, whether such a model will have a phase transition or not, all depend on the convergence of the eigenvalues at this point.

4.4 Sparse Matrix Method and Results

The first thing to do is to check for convergence. We have chosen the number of discretization points to start from $n = 40$ up to $n = 100$, and in the computation of the eigenvalues we couldn't go beyond $n = 110$. So, we have a bound due to the limitation of computational resources, which is the size of a matrix *Mathematica* can handle in this case. The Figure 4.1 shows how the eigenvalues change with the increasing number, n , of discretisation points,

Unfortunately, the eigenvalues do not converge within the range of the number of discretisation points *Mathematica* can tolerate³.

³This failure of the eigenvalues to converge might be due to the computation of K . We have already mentioned that the parameter b can make the computation of K using *Mathematica* to be impossible. This suggest that setting $b > 0$ to be less than one would be a solution. It doesn't seem to be the case though, as different parameters have been tried, but only for the above set of parameters we reported the results. We must also report that we failed to come up with a way to pin down, where exactly in this computation of K things might be going wrong. A different discretization method might be a solution here, but unfortunately we don't know better how to choose such a different because in our case it seems like passing the test of solving exactly solvable integral equations is not enough for a numerical routine to be the right choice.

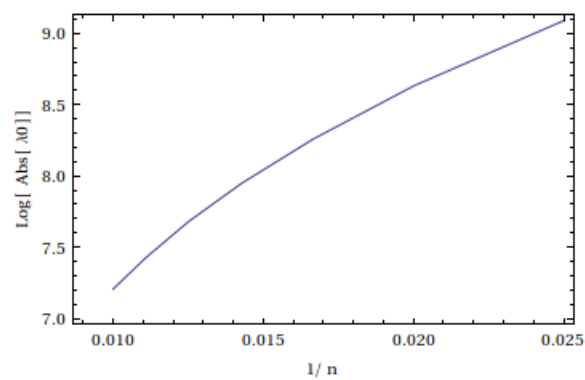


Figure 4.1: The plot of the *logarithm* of the absolute value of the largest eigenvalue, $\text{Log}|\lambda_0|$ versus the inverse of the number of discretisation points, $1/n$, for $n = 40$ to $n = 100$. We see that $\text{Log}|\lambda_0|$ does not converge, at least for as large a number of discretisation points as $n = 100$, since we can not go beyond $n = 110$.

Chapter 5

Conclusion

We had set out to generalise the Kac model's exponentially decaying potential (1.4.1) by superimposing an oscillating sinusoidal term on it (see (1.4.2)), and compute its canonical partition function (see Chapter 2). By methods similar to those used by Kac (see Appendix A), we were able to express the partition function of this generalised model in terms of the eigenvalues and eigenfunctions of the integral equation (2.2.16).

Unlike in the Kac paper, in which the integral equation is one dimensional, in our case the integral equation is two-dimensional. The integral equation is not exactly solvable, and this led to the second part of the project, the discretization of the integral equation in two dimensions and then computing the eigenvalues. Before we got to the point of computing the eigenvalues in this general case, we followed a series of steps, in which, starting from one-dimensional case we tested the discretization scheme using an exactly solvable integral equation. The eigenvalues were reproduced exactly (see Table 3.3). The one dimensional case was done because we wanted to adopt it to the two dimensional case.

We then applied the discretisation scheme to the one dimensional Kac integral equation (A.1.22), and we obtained the results in Table 3.4. We then generalised the Kac integral equation to a two dimensional case, where $K_s(x, y; \bar{x}, \bar{y}) = K_s(x, y)K(\bar{x}, \bar{y})$. From Table 3.4 we calculated the eigenvalues, for $N = 40$ discretisation points the eigenvalues are as shown in Table 3.5.

Now, in contrast to using the results in Table ?? to compute the eigenvalues of the two dimensional Kac integral equation, we have used the numerical method (3.2.3) to com-

pute the eigenvalues. The results that we obtained are shown in Table 3.6. The eigenvalues converged when increasing the number of discretisation points, exact results agreed with numerical results, and even when generalised to two dimensions we got the expected results with convergence (see Table 3.4, Table 3.5 and Table 3.6 above). This test verified that in principle the numerical method is working well.

Despite the careful construction and testing of the method, the numerical scheme failed to converge when applying it to the integral equation (2.2.16) of the generalised Kac model. This failure can be attributed to the possibility that the kernel which we derived from the generalised potential function behaves so badly that the numerically computed eigenvalues do not converge as we have already seen in Figure 4.1. By badly behaving kernel we mean that our numerical method which worked well for the Kac integral equation (eigenvalues converged for as low as $N = 40$ discretisation points) doesn't work when applied to the generalised integral equation (eigenvalues do not converge, even for as large a number of discretisation points as $N = 100$ together with an improved method, Sparse Matrix Method).

Finally, although the eigenvalues have converged for the Kac integral equation and failed to converge for the generalised integral equation, we attribute the failure of the latter to the numerical method we have used. So, we hope that with some other and better method it might be possible to decide whether the system undergoes a phase transition or not.

Appendix A

Kac Integral Equation

A.1 Derivation of the Kac Integral Equation

In this section we show the derivations of Equations (9),(10),(12), and (13) of (Kac *et al.*, 1963). The partition function for the one-dimensional gas is given by (Kac *et al.*, 1963),

$$Z(L, T, N) = \frac{1}{\Lambda^N} \frac{1}{N!} \int_0^L \cdots \int_0^L dt_1 \cdots dt_N \times \exp \left[-\frac{1}{kT} \sum_{i < j} V(|t_i - t_j|) \right] \quad (\text{A.1.1})$$

where $\Lambda^2 = h^2 / 2\pi m k T$.

Using equation (1.4.1), equation (A.1.1) becomes

$$\begin{aligned} Z(L, T, N) &= \frac{1}{\Lambda^N} \frac{1}{N!} \int_0^L \cdots \int_0^L dt_1 \cdots dt_N \\ &\times \exp \left[\nu \sum_{i < j} e^{-\gamma |t_i - t_j|} \right] \prod_{i < j} S(|t_i - t_j|) \end{aligned} \quad (\text{A.1.2})$$

where the step function $S(x)$ is defined by

$$S(x) = \begin{cases} 0 & \text{for } |x| < \delta. \\ 1 & \text{for } |x| > \delta. \end{cases} \quad (\text{A.1.3})$$

Now, let us consider

$$\begin{aligned}
\sum_{i,j=1}^N e^{-\gamma|t_i-t_j|} &= \sum_{i=1}^N e^{-\gamma|t_i-t_1|} + \sum_{i=1}^N e^{-\gamma|t_i-t_2|} + \dots + \sum_{i=1}^N e^{-\gamma|t_i-t_N|} \\
&= e^{-\gamma|t_1-t_1|} + e^{-\gamma|t_2-t_1|} + \dots + e^{-\gamma|t_N-t_1|} \\
&\quad + e^{-\gamma|t_1-t_2|} + e^{-\gamma|t_2-t_2|} + \dots + e^{-\gamma|t_N-t_2|} \\
&\quad \vdots \\
&\quad + e^{-\gamma|t_N-t_1|} + e^{-\gamma|t_N-t_2|} + \dots + e^{-\gamma|t_N-t_N|}.
\end{aligned} \tag{A.1.4}$$

Because $|t_i - t_j| = |t_j - t_i|$ and $e^{-\gamma|t_i-t_i|} = 1$ for $i = j$, equation (A.1.4) becomes

$$\sum_{i,j=1}^N e^{-\gamma|t_i-t_j|} = N + 2 \sum_{1 \leq i < j \leq N} e^{-\gamma|t_i-t_j|}. \tag{A.1.5}$$

Since the integrand in equation (A.1.2) is symmetric in the variables t_1, \dots, t_n we are going to consider the integration over the domain,

$$[0, L] \times [t_1, L] \times [t_2, L] \times \dots \times [t_N, L]$$

instead of

$$[0, L] \times [0, L] \times [0, L] \times \dots \times [0, L].$$

In that case the solution to (A.1.2) will be $N!$ times the result obtained in the case of the new domain of integration. Therefore equation (A.1.2) becomes

$$\begin{aligned}
Z(L, T, N) &= \frac{e^{-\frac{1}{2}N\nu}}{\Lambda^N} \int \dots \int_{0 < t_1 < t_2 < \dots < t_N < L} dt_1 \dots dt_N \\
&\quad \times \exp \left[\frac{\nu}{2} \sum_{i,j=1}^N e^{-\gamma|t_i-t_j|} \right] \prod_{j=1}^{N-1} S(|t_{j+1} - t_j|).
\end{aligned} \tag{A.1.6}$$

since for $t_1 < t_2 < \dots, t_N$ we have that

$$\prod_{i < j} S(|t_i - t_j|) = \prod_{j=1}^{N-1} S(|t_{j+1} - t_j|). \tag{A.1.7}$$

Appendix A

A.1. Derivation of the Kac Integral Equation

The attractive part of the integrand of equation (A.1.6) can be rewritten by using the identity

$$\begin{aligned} \exp \left[\frac{\nu}{2} \sum_{i,j=1}^N \exp(-\gamma|t_i - t_j|) \right] &= \int_{-\infty}^{\infty} \cdots \int_{-\infty}^{\infty} dx_1 \cdots dx_N \\ &\times \exp[\nu^2(x_1 + x_2 + \cdots + x_N)] \\ &\times W(x_1) \prod_{j=1}^{N-1} P(x_j|x_{j+1}, t_{j+1} - t_j), \end{aligned} \quad (\text{A.1.8})$$

where $W(x) = \frac{1}{\sqrt{2\pi}} \exp(-\frac{1}{2}x^2)$ and

$$P(x|y, t) = \frac{\exp \left\{ -\frac{(y - xe^{-\gamma t})^2}{2(1 - e^{-2\gamma t})} \right\}}{[2\pi(1 - e^{-2\gamma t})]^{\frac{1}{2}}}. \quad (\text{A.1.9})$$

Now, let

$$F_1(t_2 - t_1) = \frac{e^{-\frac{\nu}{2}}}{\Lambda} \int_{-\infty}^{\infty} dx_1 W(x_1) e^{\nu^{\frac{1}{2}} x_1} S(|t_2 - t_1|), \quad (\text{A.1.10})$$

$$\begin{aligned} F_k(t_{k+1} - t_k) &= \frac{e^{-\frac{\nu}{2}}}{\Lambda} \int_{-\infty}^{\infty} dx_k e^{\nu^{\frac{1}{2}} x_k} P(x_k|x_{k+1}; t_{k+1} - t_k) \\ &\times S(|t_{k+1} - t_k|), \end{aligned} \quad (\text{A.1.11})$$

for $k = 2, 3, \dots, N-2$, and

$$\begin{aligned} F_{N-1}(t_N - t_{N-1}) &= \frac{e^{-\frac{\nu}{2}}}{\Lambda} \int_{-\infty}^{\infty} dx_{N-1} e^{\nu^{\frac{1}{2}} x_{N-1}} \frac{e^{-\frac{\nu}{2}}}{\Lambda} \int_{-\infty}^{\infty} dx_N e^{\nu^{\frac{1}{2}} x_N} \\ &\times P(x_{N-1}|x_N; t_N - t_{N-1}) \\ &\times S(|t_N - t_{N-1}|). \end{aligned} \quad (\text{A.1.12})$$

Substituting equation (A.1.8) into equation (A.1.7) and making a Laplace transformation in L , we obtain

$$\begin{aligned} \mathcal{Z}(s, T, N) &= \int_0^{\infty} e^{-sL} Z(L, T, N) dL \\ &= \int_0^{\infty} dL e^{-sL} \int_0^L dt_1 \int_{t_1}^L dt_2 \int_{t_2}^L dt_3 \cdots \int_{t_{N-1}}^L dt_N \prod_{j=1}^{N-1} F_j(t_{j+1} - t_j) \\ &= \int_0^{\infty} dt_1 \int_{t_1}^{\infty} dt_2 \cdots \int_{t_{N-1}}^{\infty} dt_N \int_{t_N}^{\infty} dL e^{-sL} \prod_{j=1}^{N-1} F_j(t_{j+1} - t_j) \end{aligned} \quad (\text{A.1.13})$$

Now, we make change of variables,

$$\begin{aligned} t_1 &= \tau_1, \\ t_2 &= \tau_1 + \tau_2, \\ &\dots \\ t_N &= \tau_1 + \tau_2 + \dots + \tau_N, \\ L &= \tau_1 + \tau_2 + \dots + \tau_N + \tau_{N+1}. \end{aligned}$$

We have to find the Jacobian so that we can write the integral in terms of the new variables τ_i . First we note that $F_j(t_{j+1} - t_j) = F_j(\tau_{j+1})$. The Jacobian is

$$\frac{\partial(t_1, t_2, \dots, t_{N+1})}{\partial(\tau_1, \tau_2, \dots, \tau_{N+1})} = \begin{vmatrix} \frac{\partial t_1}{\partial \tau_1} & \frac{\partial t_1}{\partial \tau_2} & \dots & \frac{\partial t_1}{\partial \tau_{N+1}} \\ \frac{\partial t_2}{\partial \tau_1} & \frac{\partial t_2}{\partial \tau_2} & \dots & \frac{\partial t_2}{\partial \tau_{N+1}} \\ \vdots & \vdots & \ddots & \vdots \\ \frac{\partial t_N}{\partial \tau_1} & \frac{\partial t_N}{\partial \tau_2} & \dots & \frac{\partial t_N}{\partial \tau_{N+1}} \\ \frac{\partial L}{\partial \tau_1} & \frac{\partial L}{\partial \tau_2} & \dots & \frac{\partial L}{\partial \tau_{N+1}} \end{vmatrix} = \begin{vmatrix} 1 & 0 & \dots & 0 \\ 1 & 1 & \dots & 0 \\ \vdots & \vdots & \ddots & \vdots \\ 1 & 1 & \dots & 1 \end{vmatrix} = 1. \quad (\text{A.1.14})$$

Also, to find the new limits of integration we use $t_1 \leq t_2 \leq \dots \leq t_N \leq t_{N+1}$. The first inequality and the limits of integration of t_1 tells us that when $t_1 = 0$, we have that $\tau_1 = 0$ and $t_1 = \infty$, $\tau_1 = \infty$, and using the inequalities we have that $t_1 \leq t_2$, which implies $\tau_1 \leq \tau_1 + \tau_2$ or $0 \leq \tau_2$. Proceeding in this manner all the inequalities gives us $0 \leq \tau_i$ for $i = 1, 2, \dots, N, N+1$.

Now, using the change of variables and the Jacobian in equation (A.1.14) the integral

Appendix A

A.1. Derivation of the Kac Integral Equation

equation (A.1.13) becomes

$$\begin{aligned}
 \mathcal{Z}(s, T, N) &= \int_0^\infty d\tau_1 \int_0^\infty d\tau_2 \cdots \int_0^\infty d\tau_N \int_0^\infty d\tau_{N+1} \\
 &\quad \times e^{-s(\tau_1 + \tau_2 + \cdots + \tau_N + \tau_{N+1})} \prod_{j=1}^{N-1} F_j(\tau_{j+1}) \\
 &= \int_0^\infty d\tau_1 e^{-s\tau_1} \int_0^\infty d\tau_2 \cdots \int_0^\infty d\tau_N \int_0^\infty d\tau_{N+1} e^{-s\tau_{N+1}} \\
 &\quad \times e^{-s(\tau_2 + \cdots + \tau_N)} \prod_{j=1}^{N-1} F_j(\tau_{j+1}) \\
 &= \int_0^\infty d\tau_1 e^{-s\tau_1} \int_0^\infty d\tau_2 e^{-s\tau_2} F_1(\tau_2) \int_0^\infty d\tau_3 e^{-s\tau_3} F_2(\tau_3) \\
 &\quad \cdots \int_0^\infty d\tau_N e^{-s\tau_N} F_{N-1}(\tau_N) \int_0^\infty d\tau_{N+1} e^{-s\tau_{N+1}} \quad (A.1.15)
 \end{aligned}$$

and

$$\int_0^\infty d\tau_1 e^{-s\tau_1} = \int_0^\infty d\tau_{N+1} e^{-s\tau_{N+1}} = \frac{1}{s}.$$

Therefore, we have

$$\mathcal{Z}(s, T, N) = \frac{1}{s^2} \prod_{j=1}^{N-1} \int_0^\infty d\tau e^{-s\tau_{j+1}} F_j(\tau_{j+1}). \quad (A.1.16)$$

Putting the appropriate $F_k(\tau_{k+1})$ into equation (A.1.16) we get

$$\begin{aligned}
 \mathcal{Z}(s, T, N) &= \frac{e^{-Nv/2}}{\Lambda^N s^2} \int_{-\infty}^\infty \cdots \int_{-\infty}^\infty dx_1 \cdots dx_N \\
 &\quad \times \exp \left[\nu^{\frac{1}{2}} (x_1 + \cdots + x_N) \right] W(x_1) \prod_{i=1}^{N-1} p_s(x_i | x_{i+1}), \quad (A.1.17)
 \end{aligned}$$

where

$$\begin{aligned}
 p_s(x|y) &= \int_0^\infty \exp(-st) P(x|y; t) S(t) dt \\
 &= \int_\delta^\infty \exp(-st) P(x|y; t) dt. \quad (A.1.18)
 \end{aligned}$$

From equation (A.1.17) we have

$$\begin{aligned}
& \exp \left[\nu^{\frac{1}{2}}(x_1 + \cdots + x_N) \right] \prod_{i=1}^{N-1} p_s(x_i | x_{i+1}) \\
&= \exp \left(\frac{\nu^{\frac{1}{2}}}{2} x_1 \right) p_s(x_1 | x_2) \exp \left[\frac{\nu^{\frac{1}{2}}}{2} (x_1 + x_2) \right] \\
&\quad \times p_s(x_2 | x_3) \exp \left[\frac{\nu^{\frac{1}{2}}}{2} (x_2 + x_3) \right] \\
&\quad \times p_s(x_3 | x_4) \exp \left[\frac{\nu^{\frac{1}{2}}}{2} (x_3 + x_4) \right] \\
&\quad \vdots \\
&\quad \times p_s(x_{N-1} | x_N) \exp \left[\frac{\nu^{\frac{1}{2}}}{2} (x_{N-1} + x_N) \right] \exp \left(\frac{\nu^{\frac{1}{2}}}{2} x_N \right) \\
&= \exp \left[\frac{\nu^{\frac{1}{2}}}{2} (x_1 + x_N) \right] \prod_{j=1}^{N-1} p_s(x_j | x_{j+1}) \exp \left[\frac{\nu^{\frac{1}{2}}}{2} (x_j + x_{j+1}) \right] \\
&= \exp \left[\frac{\nu^{\frac{1}{2}}}{2} (x_1 + x_N) \right] \frac{W(x_1)}{W(x_1)^{\frac{1}{2}} W(x_2)^{\frac{1}{2}}} \\
&\quad \times p_s(x_1 | x_2) \exp \left[\frac{\nu^{\frac{1}{2}}}{2} (x_1 + x_2) \right] \\
&\quad \times \frac{W(x_2)}{W(x_2)^{\frac{1}{2}} W(x_3)^{\frac{1}{2}}} p_s(x_2 | x_3) \exp \left[\frac{\nu^{\frac{1}{2}}}{2} (x_2 + x_3) \right] \\
&\quad \times \frac{W(x_3)}{W(x_3)^{\frac{1}{2}} W(x_4)^{\frac{1}{2}}} p_s(x_3 | x_4) \exp \left[\frac{\nu^{\frac{1}{2}}}{2} (x_3 + x_4) \right] \\
&\quad \vdots \\
&\quad \times \frac{W(x_{N-1})}{W(x_{N-1})^{\frac{1}{2}} W(x_N)^{\frac{1}{2}}} p_s(x_{N-1} | x_N) \exp \left[\frac{\nu^{\frac{1}{2}}}{2} (x_{N-1} + x_N) \right] W(x_N)^{\frac{1}{2}} \\
&= \exp \left[\frac{\nu^{\frac{1}{2}}}{2} (x_1 + x_N) \right] W(x_1)^{\frac{1}{2}} W(x_N)^{\frac{1}{2}} \prod_{j=1}^{N-1} K_s(x_j, x_{j+1}) \tag{A.1.19}
\end{aligned}$$

with

$$K_s(x_i, x_{i+1}) = \frac{W(x_i) p_s(x_i | x_{i+1})}{[W(x_i) W(x_{i+1})]^{\frac{1}{2}}} \exp \left[\frac{\nu^{\frac{1}{2}}}{2} (x_i + x_{i+1}) \right]. \tag{A.1.20}$$

Therefore equation (A.1.17) becomes

$$\begin{aligned} \mathcal{Z}(s, T, N) &= \frac{e^{-N\nu/2}}{\Lambda^{Ns^2}} \int_{-\infty}^{\infty} \cdots \int_{-\infty}^{\infty} dx_1 \cdots dx_N \\ &\times \exp \left[\frac{\nu^{\frac{1}{2}}}{2} (x_1 + x_N) \right] W(x_1)^{\frac{1}{2}} W(x_N)^{\frac{1}{2}} \prod_{j=1}^{N-1} K_s(x_j, x_{j+1}) \end{aligned} \quad (\text{A.1.21})$$

From now, we consider the function K_s as the kernel of the so-called Kac integral equation

$$\int_{-\infty}^{\infty} K_s(x, y) \psi(y) dy = \lambda \psi(x). \quad (\text{A.1.22})$$

A.2 Properties of the Kernel

This section serves to show some properties of the kernel. Firstly, we have that the kernel $K_s(x, y)$ is symmetric, that is $K_s(x, y) = K_s(y, x)$. According to equation (4.8) of (Kac, 1959), the kernel K_s in (A.1.20) can be written in the form

$$\begin{aligned} K_s(x, y) &= \exp \left[\frac{\nu^{\frac{1}{2}}(x + y)}{2} \right] \\ &\times \sum_{k=0}^{\infty} \frac{\exp(-x^2/2) H_k(x) \exp(-y^2/2) H_k(y)}{2\pi k!} \exp(-k\gamma t) \\ &\times \int_{\delta}^{\infty} \exp(-st) \exp(-k\gamma t) dt. \end{aligned} \quad (\text{A.2.1})$$

From equation (A.2.1) we see that $K_s(x, y)$ is symmetric.

We also have that the following two conditions for the kernel are true:

(a) $K_s(x, y)$ is positive definite, which means that

$$\int \int K_s(x, y) \psi(x) \psi(y) dx dy \quad (\text{A.2.2})$$

is always positive, whenever $\psi(x)$ is not identically 0 (for a proof see (Kac, 1959));

(b) $K_s(x, y)$ is a Hilbert-Schmidt kernel, which means that

$$\int \int K_s^2(x, y) dx dy < \infty. \quad (\text{A.2.3})$$

From these facts, using the Hilbert-Schmidt theory, one can conclude that equation (A.1.22) has a discrete set of positive eigenvalues $\lambda_i(s)$ starting from a maximum eigenvalue $\lambda_0(s)$ and converging to zero as $i \rightarrow \infty$, that the corresponding eigenfunctions

$\psi_i(x, s)$ form a complete orthonormal set, and that the kernel $K_s(x, y)$ can be expanded in the series

$$K_s(x, y) = \sum_{i=0}^{\infty} \lambda_i(s) \psi_i(x, s) \psi_i(y, s). \quad (\text{A.2.4})$$

Inserting equation (A.2.4) into equation (A.1.21) we get

$$\begin{aligned} \mathcal{Z}(s, T, N) &= \frac{e^{-N\nu/2}}{\Lambda^N s^2} \int_{-\infty}^{\infty} \cdots \int_{-\infty}^{\infty} dx_1 \cdots dx_N \\ &\quad \times \exp \left[\frac{\nu^{\frac{1}{2}}}{2} (x_1 + x_N) \right] W(x_1)^{\frac{1}{2}} W(x_N)^{\frac{1}{2}} \\ &\quad \times \prod_{j=1}^{N-1} \left[\sum_{j=0}^{\infty} \lambda_j(s) \psi_j(x, s) \psi_j(y, s) \right] \end{aligned} \quad (\text{A.2.5})$$

Now, suppressing s , we are going to integrate equation (A.2.5) over $x_2 \cdots x_{N-1}$. Let us consider

$$\begin{aligned} &\int_{-\infty}^{\infty} \cdots \int_{-\infty}^{\infty} dx_1 \cdots dx_N \exp \left[\frac{\nu^{\frac{1}{2}}}{2} (x_1 + x_N) \right] W(x_1)^{\frac{1}{2}} W(x_N)^{\frac{1}{2}} \prod_{j=1}^{N-1} \left[\sum_{j=0}^{\infty} \lambda_j \psi_j(x) \psi_j(y) \right] \\ &= \int_{-\infty}^{\infty} dx_1 W(x_1)^{\frac{1}{2}} \exp \left(\frac{x_1 \nu^{\frac{1}{2}}}{2} \right) \\ &\quad \times \int_{-\infty}^{\infty} \cdots \int_{-\infty}^{\infty} \left(\sum_{j_1=0}^{\infty} \lambda_{j_1} \psi_{j_1}(x_1) \psi_{j_1}(x_2) \right) \\ &\quad \times \left(\sum_{j_2=0}^{\infty} \lambda_{j_2} \psi_{j_2}(x_2) \psi_{j_2}(x_3) \right) \\ &\quad \times \left(\sum_{j_3=0}^{\infty} \lambda_{j_3} \psi_{j_3}(x_3) \psi_{j_3}(x_4) \right) \\ &\quad \vdots \\ &\quad \times \left(\sum_{j_{N-1}=0}^{\infty} \lambda_{j_{N-1}} \psi_{j_{N-1}}(x_{N-1}) \psi_{j_{N-1}}(x_N) \right) \\ &\quad \times W(x_N)^{\frac{1}{2}} \exp \left(\frac{x_N \nu^{\frac{1}{2}}}{2} \right) \\ &\quad \times dx_2 \cdots dx_{N-1} dx_N. \end{aligned} \quad (\text{A.2.6})$$

Appendix A

A.2. Properties of the Kernel

The right hand side of equation (A.2.6) without

$$\int_{-\infty}^{\infty} dx_1 W(x_1)^{\frac{1}{2}} \psi_{j_1} \exp\left(\frac{x_1 \nu^{\frac{1}{2}}}{2}\right) \quad (\text{A.2.7})$$

and

$$\int_{-\infty}^{\infty} dx_N W(x_N)^{\frac{1}{2}} \psi_{j_N} \exp\left(\frac{x_N \nu^{\frac{1}{2}}}{2}\right) \quad (\text{A.2.8})$$

becomes

$$\begin{aligned} & \sum_{j_1, j_2, j_3, \dots, j_{N-1}} \lambda_{j_1} \lambda_{j_2} \cdots \lambda_{j_{N-1}} \int_{-\infty}^{\infty} dx_2 \psi_{j_1}(x_2) \psi_{j_2}(x_2) \\ & \times \int_{-\infty}^{\infty} dx_3 \psi_{j_2}(x_3) \psi_{j_3}(x_3) \int_{-\infty}^{\infty} dx_4 \psi_{j_3}(x_4) \psi_{j_4}(x_4) \\ & \times \int_{-\infty}^{\infty} dx_5 \psi_{j_4}(x_5) \psi_{j_5}(x_5) \int_{-\infty}^{\infty} dx_6 \psi_{j_5}(x_6) \psi_{j_6}(x_6) \\ & \vdots \\ & \times \int_{-\infty}^{\infty} dx_{N-1} \psi_{j_{N-2}}(x_{N-1}) \psi_{j_{N-1}}(x_{N-1}) \\ & = \sum_{j_1, j_2, j_3, \dots, j_{N-1}} \lambda_{j_1} \lambda_{j_2} \lambda_{j_3} \cdots \lambda_{j_{N-1}} \delta_{j_1, j_2} \delta_{j_2, j_3} \delta_{j_3, j_4} \cdots \delta_{j_{N-2}, j_{N-1}} \\ & = \sum_{j_1, j_3, \dots, j_{N-1}} \lambda_{j_1}^2 \lambda_{j_3} \cdots \lambda_{j_{N-1}} \delta_{j_1, j_3} \delta_{j_3, j_4} \cdots \delta_{j_{N-2}, j_{N-1}} \\ & = \sum_{j_1, j_4, \dots, j_{N-1}} \lambda_{j_1}^3 \lambda_{j_4} \cdots \lambda_{j_{N-1}} \delta_{j_1, j_4} \cdots \delta_{j_{N-2}, j_{N-1}} \\ & \vdots \\ & = \sum_{j_1} \lambda_{j_1}^{N-1}. \end{aligned} \quad (\text{A.2.9})$$

Using (A.2.7), (A.2.8) and (A.2.9) equation (A.2.5) becomes

$$\begin{aligned} \mathcal{Z}(s, T, N) &= \frac{e^{-\frac{N\nu}{2}}}{\Lambda^N s^2} \sum_{j=1}^{\infty} \lambda_j^{N-1} \left[\int_{-\infty}^{\infty} dx_1 W(x_1)^{\frac{1}{2}} \psi_j(x_1) \exp\left(\frac{x_1 \nu^{\frac{1}{2}}}{2}\right) \right] \\ & \times \left[\int_{-\infty}^{\infty} dx_N W(x_N)^{\frac{1}{2}} \psi_j(x_N) \exp\left(\frac{x_N \nu^{\frac{1}{2}}}{2}\right) \right] \\ &= \frac{e^{-\frac{N\nu}{2}}}{\Lambda^N s^2} \sum_{j=1}^{\infty} \lambda_j^{N-1}(s) A_j^2 \end{aligned} \quad (\text{A.2.10})$$

with

$$A_j = \int_{-\infty}^{\infty} dx W(x)^{\frac{1}{2}} \psi_j(x) \exp\left(\frac{x\nu^{\frac{1}{2}}}{2}\right). \quad (\text{A.2.11})$$

Equation (A.2.10) is the Laplace transform of the partition function in terms of the eigenvalues of the Kac integral operator, which is the main result we have set out to find as we have already mentioned in the introduction. Again, this is similar in spirit to what is done in the transfer matrix approach mentioned before.

Appendix B

Hilbert-Schmidt Property of kernel

We now prove that

$$K_s(x, y; \bar{x}, \bar{y}) = \frac{W(x)W(y)p_s(x, y; \bar{x}, \bar{y})}{[W(x)W(y)W(\bar{x})W(\bar{y})]^{1/2}} \times \exp \left\{ \left[\nu^{1/2}(x + \bar{x}) + (\nu^*)^{1/2}(y + \bar{y}) \right] \right\} \quad (\text{B.0.1})$$

which is symmetric upon exchanging (x, y) with (\bar{x}, \bar{y}) , is a Hilbert-Schmidt kernel, that is,

$$\int \int \int \int_{-\infty}^{\infty} dx dy d\bar{x} d\bar{y} |K_s(x, y; \bar{x}, \bar{y})|^2 < \infty \quad (\text{B.0.2})$$

PROOF:

We have

$$\begin{aligned}
& \int \int \int \int_{-\infty}^{\infty} dx dy d\bar{x} d\bar{y} |K_s(x, y; \bar{x}, \bar{y})|^2 \\
&= \int \int \int \int_{-\infty}^{\infty} dx dy d\bar{x} d\bar{y} K_s(x, y; \bar{x}, \bar{y}) K_s^*(\bar{x}, \bar{y}; x, y) \\
&= \int \int \int \int_{-\infty}^{\infty} dx dy d\bar{x} d\bar{y} p_s(x, y; \bar{x}, \bar{y}) p_s^*(\bar{x}, \bar{y}; x, y) \\
&\quad \times \exp \left\{ \left[\nu^{1/2}(x + \bar{x}) + (\nu^*)^{1/2}(y + \bar{y}) \right] / 2 \right\} \\
&\quad \times \exp \left\{ \left[(\nu^{1/2})^*(\bar{x} + x) + ((\nu^*)^{1/2})^*(\bar{y} + y) \right] / 2 \right\} \\
&= \int \int_{\delta}^{\infty} d\tau_1 d\tau_2 e^{-s(\tau_1 + \tau_2)} \int \int_{-\infty}^{\infty} dx d\bar{x} P_{\gamma}(x|\bar{x}, \tau_1) P_{\gamma}^*(\bar{x}|x, \tau_2) \\
&\quad \times \exp \left\{ \left[[\nu^{1/2} + (\nu^{1/2})^*](x + \bar{x}) \right] / 2 \right\} \\
&\quad \int \int_{-\infty}^{\infty} dy d\bar{y} P_{\gamma^*}(\bar{y}|y, \tau_1) P_{\gamma^*}^*(y|\bar{y}, \tau_2) \\
&\quad \times \exp \left\{ \left[[(\nu^*)^{1/2} + ((\nu^*)^{1/2})^*](y + \bar{y}) \right] / 2 \right\}
\end{aligned} \tag{B.0.3}$$

From (B.0.3) we see that we simply have to show that

$$\int \int_{-\infty}^{\infty} dy d\bar{y} P_{\gamma^*}(\bar{y}|y, \tau_1) P_{\gamma^*}^*(y|\bar{y}, \tau_2) \times \exp \left\{ \left[[(\nu^*)^{1/2} + ((\nu^*)^{1/2})^*](y + \bar{y}) \right] / 2 \right\}$$

is finite, to conclude that the kernel satisfies (B.0.2).

By Cauchy-Schwartz,

$$\begin{aligned}
& \int \int_{-\infty}^{\infty} dx d\bar{x} P_{\gamma}(x|\bar{x}, \tau_1) P_{\gamma}^*(\bar{x}|x, \tau_2) \exp \left\{ \left[[\nu^{1/2} + (\nu^{1/2})^*](x + \bar{x}) \right] / 2 \right\} \\
&\leq \left(\int \int_{-\infty}^{\infty} dx d\bar{x} \frac{W(x)}{W(\bar{x})} \left| P_{\gamma}(x|\bar{x}, \tau_1) \exp \left\{ [\nu^{1/2} + (\nu^{1/2})^*](x + \bar{x}) \right\} \right|^2 \right)^{1/2} \\
&\quad \times \left(\int \int_{-\infty}^{\infty} dx d\bar{x} \frac{W(\bar{x})}{W(x)} \left| P_{\gamma}^*(\bar{x}|x, \tau_2) \exp \left\{ [\nu^{1/2} + (\nu^{1/2})^*](x + \bar{x}) \right\} \right|^2 \right)^{1/2}
\end{aligned} \tag{B.0.4}$$

which reduces the problem to only showing that

$$\int \int_{-\infty}^{\infty} dx d\bar{x} \frac{W(\bar{x})}{W(x)} \left| P_{\gamma}^*(\bar{x}|x, \tau_2) \exp \left\{ [\nu^{1/2} + (\nu^{1/2})^*](x + \bar{x}) \right\} \right|^2$$

Appendix A

is finite. The latter expression can be written more explicitly as follows

$$\begin{aligned}
 & \int \int_{-\infty}^{\infty} dx d\bar{x} \frac{W(x)}{W(\bar{x})} \left| P_{\gamma}(x|\bar{x}, \tau) \exp \left\{ [\nu^{1/2} + (\nu^{1/2})^*](x + \bar{x}) \right\} \right|^2 \\
 &= \int \int_{-\infty}^{\infty} dx d\bar{x} \frac{W(x)}{W(\bar{x})} |P_{\gamma}(x|\bar{x}, \tau)|^2 \exp \left\{ 2[\nu^{1/2} + (\nu^{1/2})^*](x + \bar{x}) \right\} \\
 &= \int \int_{-\infty}^{\infty} dx d\bar{x} \frac{W(x)}{W(\bar{x})} P_{\gamma}(x|\bar{x}, \tau) P_{\gamma}^*(x|\bar{x}, \tau) \exp \left\{ 2[\nu^{1/2} + (\nu^{1/2})^*](x + \bar{x}) \right\}
 \end{aligned} \tag{B.0.5}$$

Now,

$$\begin{aligned}
 & P_{\gamma}(x|\bar{x}, \tau) P_{\gamma}^*(x|\bar{x}, \tau) \\
 &= \frac{1}{\sqrt{2\pi(1 - e^{-2\gamma\tau})}} \exp \left\{ -\frac{(\bar{x} - xe^{-\gamma\tau})^2}{2(1 - e^{-2\gamma\tau})} \right\} \left[\frac{1}{\sqrt{2\pi(1 - e^{-2\gamma^*\tau})}} \right]^* \exp \left\{ -\frac{(\bar{x} - xe^{-\gamma^*\tau})^2}{2(1 - e^{-2\gamma^*\tau})} \right\} \\
 &= \frac{1}{\sqrt{2\pi(1 - e^{-2\gamma\tau})}} \left[\frac{1}{\sqrt{2\pi(1 - e^{-2\gamma^*\tau})}} \right]^* \exp \left\{ -\frac{(\bar{x} - xe^{-\gamma^*\tau})^2}{2(1 - e^{-2\gamma^*\tau})} - \frac{(\bar{x} - xe^{-\gamma\tau})^2}{2(1 - e^{-2\gamma\tau})} \right\}
 \end{aligned} \tag{B.0.6}$$

Simplifying the latter expression,

$$\begin{aligned}
 & \exp \left\{ -\frac{(\bar{x} - xe^{-\gamma\tau})^2}{2(1 - e^{-2\gamma\tau})} - \frac{(\bar{x} - xe^{-\gamma^*\tau})^2}{2(1 - e^{-2\gamma^*\tau})} \right\} \\
 &= \exp \left(\frac{2(1 - e^{-2\gamma^*\tau})[-\bar{x}^2 + 2\bar{x}xe^{-\gamma\tau} + x^2e^{-2\gamma\tau}]}{2(1 - e^{-2\gamma\tau}) \times 2(1 - e^{-2\gamma^*\tau})} \right) \\
 &\times \exp \left(\frac{2(1 - e^{-2\gamma\tau})[-\bar{x}^2 + 2\bar{x}xe^{-\gamma^*\tau} + x^2e^{-2\gamma^*\tau}]}{2(1 - e^{-2\gamma\tau}) \times 2(1 - e^{-2\gamma^*\tau})} \right) \\
 &= \exp \left(-\frac{2(1 - e^{-2\gamma^*\tau}) + 2(1 - e^{-2\gamma\tau})}{2(1 - e^{-2\gamma\tau}) \times 2(1 - e^{-2\gamma^*\tau})} \bar{x}^2 \right) \\
 &\times \exp \left(\frac{2(1 - e^{-2\gamma^*\tau})e^{-\gamma\tau} + 2(1 - e^{-2\gamma\tau})e^{-\gamma^*\tau}}{2(1 - e^{-2\gamma\tau}) \times 2(1 - e^{-2\gamma^*\tau})} (2\bar{x}x) \right) \\
 &\times \exp \left(-\frac{2(1 - e^{-2\gamma^*\tau})e^{-2\gamma\tau} + 2(1 - e^{-2\gamma\tau})e^{-2\gamma^*\tau}}{2(1 - e^{-2\gamma\tau}) \times 2(1 - e^{-2\gamma^*\tau})} x^2 \right) \\
 &= \exp(-p\bar{x}^2 + 2q\bar{x}x - rx^2)
 \end{aligned} \tag{B.0.7}$$

where

$$p = \frac{2(1 - e^{-2\gamma^*\tau}) + 2(1 - e^{-2\gamma\tau})}{2(1 - e^{-2\gamma\tau}) \times 2(1 - e^{-2\gamma^*\tau})}, \tag{B.0.8}$$

$$q = \frac{2(1 - e^{-2\gamma^*\tau})e^{-\gamma\tau} + 2(1 - e^{-2\gamma\tau})e^{-\gamma^*\tau}}{2(1 - e^{-2\gamma\tau}) \times 2(1 - e^{-2\gamma^*\tau})}, \text{ and} \quad (\text{B.0.9})$$

$$r = \frac{2(1 - e^{-2\gamma^*\tau})e^{-2\gamma\tau} + 2(1 - e^{-2\gamma\tau})e^{-2\gamma^*\tau}}{2(1 - e^{-2\gamma\tau}) \times 2(1 - e^{-2\gamma^*\tau})} \quad (\text{B.0.10})$$

Now, the RHS of (B.0.5) becomes

$$\begin{aligned} & \int \int_{-\infty}^{\infty} dx d\bar{x} \frac{W(x)}{W(\bar{x})} P_{\gamma}(x|\bar{x}, \tau) P_{\gamma}^*(x|\bar{x}, \tau) \exp \left\{ 2[\nu^{1/2} + (\nu^{1/2})^*](x + \bar{x}) \right\} \\ &= \frac{1}{\sqrt{2\pi(1 - e^{-2\gamma\tau})}} \left[\frac{1}{\sqrt{2\pi(1 - e^{-2\gamma\tau})}} \right]^* \\ & \times \int \int_{-\infty}^{\infty} dx d\bar{x} \exp \left(\frac{-x^2 + \bar{x}^2}{2} \right) \exp(-p\bar{x}^2 + 2q\bar{x}x - rx^2) \exp(\zeta(x + \bar{x})) \\ &= \frac{1}{\sqrt{2\pi(1 - e^{-2\gamma\tau})}} \left[\frac{1}{\sqrt{2\pi(1 - e^{-2\gamma\tau})}} \right]^* \int_{-\infty}^{\infty} dx \exp \left(-\frac{x^2}{2} - rx^2 + \zeta x \right) \\ & \times \int_{-\infty}^{\infty} d\bar{x} \exp \left(\frac{\bar{x}^2}{2} - p\bar{x}^2 + (2qx + \zeta)\bar{x} \right) \\ &= \frac{1}{\sqrt{2\pi(1 - e^{-2\gamma\tau})}} \left[\frac{1}{\sqrt{2\pi(1 - e^{-2\gamma\tau})}} \right]^* \sqrt{\frac{\pi}{(\frac{1}{2} - p)}} \\ & \times \int_{-\infty}^{\infty} dx \exp \left(-\left(\frac{1}{2} + r \right) x^2 + \zeta x \right) \exp \left\{ \frac{(2qx + \zeta)^2}{4(p - \frac{1}{2})} \right\} \\ &= \frac{1}{\sqrt{2\pi(1 - e^{-2\gamma\tau})}} \left[\frac{1}{\sqrt{2\pi(1 - e^{-2\gamma\tau})}} \right]^* \sqrt{\frac{\pi}{(p - \frac{1}{2})}} \exp \left(\frac{\zeta^2}{4(p - \frac{1}{2})} \right) \\ & \times \int_{-\infty}^{\infty} dx \exp \left\{ -\left(\left(\frac{1}{2} + r \right) - \frac{q^2}{(p - \frac{1}{2})} \right) x^2 + \zeta \left(1 + \frac{q}{(p - \frac{1}{2})} \right) x \right\} \\ &= \frac{1}{\sqrt{2\pi(1 - e^{-2\gamma\tau})}} \left[\frac{1}{\sqrt{2\pi(1 - e^{-2\gamma\tau})}} \right]^* \sqrt{\frac{\pi}{(p - \frac{1}{2})}} \exp \left(\frac{\zeta^2}{4(p - \frac{1}{2})} \right) \\ & \times \sqrt{\frac{\pi}{(\frac{1}{2} + r) - \frac{q^2}{(p - \frac{1}{2})}}} \exp \left\{ \frac{\zeta^2 \left(1 + \frac{q}{(p - \frac{1}{2})} \right)^2}{4 \left((\frac{1}{2} + r) - \frac{q^2}{(p - \frac{1}{2})} \right)} \right\} \end{aligned} \quad (\text{B.0.11})$$

Appendix A

where

$$\xi = 2[v^{1/2} + (v^{1/2})^*] \quad (\text{B.0.12})$$

Since RHS of (B.0.11) is finite for $0 < \tau < \infty$. It therefore follows from the integration of this product of RHS of (B.0.11) and e^{-st} that the kernel is indeed a Hilbert-Schmidt kernel.

List of References

- Kac, M.: On the partition function of a one-dimensional gas. *Physics of Fluids*, vol. 2, p. 8, 1959.
- Salinas, S.: *Introduction to statistical physics*. Springer, 2013.
- Nishimori, H. and Ortiz, G.: *Elements of phase transitions and critical phenomena*. Oxford University Press, 2010.
- M. Blaber: Chemical kinetics. CHM1046, http://www.mikeblaber.org/oldwine/chm1046/p_exams/exam1b/exam1key.htm, Accessed October 09, 2015.
- Kastner, M.: *On the origin of phase transitions in long-and short-range interacting systems*. in: Long-Range Interacting Systems. Lecture Notes of the Les Houches Summer School: Volume 90, August 2008, pp. 329–346, editors: T. Dauxois, S. Ruffo, and L. F. Cugliandolo, Oxford University Press, 2010.
- Ising, E.: Beitrag zur Theorie des Ferromagnetismus. *Zeitschrift für Physik*, vol. 31, no. 1, pp. 253–258, 1925.
- Yeomans, J.M.: *Statistical mechanics of phase transitions*. Oxford University Press, 1992.
- Müller-Nedebock, K.: *Study guide; Statistical Physics B; Physics 721*. University of Stellenbosch, 2014.
- Kac, M., Uhlenbeck, G. and Hemmer, P.: On the van der Waals theory of the vapor-liquid equilibrium. I. Discussion of a one-dimensional model. *Journal of Mathematical Physics*, vol. 4, p. 216, 1963.
- Flannery, B.P., Press, W.H., Teukolsky, S.A. and Vetterling, W.: *Numerical recipes in C*. Cambridge University Press, 1992.
- Masujima, M.: *Applied Mathematical Methods in Theoretical Physics*. Wiley Online Library, 2005.